

# The molecular systems composed of the charmed mesons in the $H\bar{S} + h.c.$ doublet

Lei-Lei Shen, Xiao-Lin Chen,\* Zhi-Gang Luo, Peng-Zhi Huang, and Shi-Lin Zhu†  
*Department of Physics and State Key Laboratory of Nuclear Physics and Technology  
and Center of High Energy Physics, Peking University, Beijing 100871, China*

Peng-Fei Yu and Xiang Liu‡§  
*School of Physical Science and Technology, Lanzhou University, Lanzhou 730000, China*  
(Dated: November 10, 2018)

We study the possible heavy molecular states composed of a pair of charm mesons in the H and S doublets. Since the P-wave charm-strange mesons  $D_{s0}(2317)$  and  $D_{s1}(2460)$  are extremely narrow, the future experimental observation of the possible heavy molecular states composed of  $D_s/D_s^*$  and  $D_{s0}(2317)/D_{s1}(2460)$  may be feasible if they really exist. Especially the possible  $J^{PC} = 1^{--}$  states may be searched for via the initial state radiation technique.

PACS numbers: 12.39.-x, 13.75.Lb, 13.20.Jf

## I. INTRODUCTION

The new family of the charmonium or charmonium-like states include  $X(3872)$ ,  $Y(3940)$ ,  $Y(4260)$ ,  $Z(3930)$ ,  $X(3940)$ ,  $Y(4325)$ ,  $Y(4360)$ ,  $Y(4660)$ ,  $Z^+(4430)$ ,  $Z^+(4050)$ ,  $Z^+(4250)$  and  $Y(4140)$  etc [1–11]. Many states sit on the the threshold of two charmed mesons, which inspired some of them (especially those charged ones) to be candidates of heavy molecules [12–20].

In the heavy quark limit, the S-wave and P-wave heavy mesons can be categorized into three doublets:  $H = (0^-, 1^-)$ ,  $S = (0^+, 1^+)$ ,  $T = (1^+, 2^+)$ . We collect their masses from PDG in Table I. The bottom mesons in the  $S$  doublet are still missing experimentally. Thus, we will adopt the theoretical predictions of the bottom meson masses in the  $S$  doublet when we study the heavy flavor molecular system composed of the bottom and anti-bottom mesons.

In the framework of the meson exchange model, we have investigated the possible loosely bound molecular states composed of a pair of heavy mesons in Refs. [16–21]. In this work, we will investigate the possible heavy molecular system constructed by the charmed and anti-charmed mesons, where one meson is in the  $H$  doublet and the other one is in the  $S$  doublet. In the following, we denote the heavy flavor molecular system as the  $H\bar{S} + h.c.$  system for the convenience.

The  $H\bar{S} + h.c.$  system can be categorized into four subsystems:  $[PP_0^*]$ ,  $[PP_1']$ ,  $[P^*P_0^*]$  and  $[P^*P_1']$ . They correspond to different quantum number combinations  $0^- + 0^+$ ,  $0^- + 1^+$ ,  $1^- + 0^+$  and  $1^- + 1^+$ , respectively. Since charmed mesons belong to the fundamental representation of flavor  $SU(3)$ , the system constructed by the charmed meson and anti-charmed meson forms an octet and a singlet:  $3 \otimes \bar{3} = 8 \oplus 1$  as illustrated in Table II. The parameter  $c = \mp 1$  in the flavor wave functions corresponds to the charge parity  $C = \pm 1$  respectively for the neutral systems as pointed out in Refs. [16–19].

This paper is organized as follows. We review the formalism in Section II and present the results in Section III. The last section is a short summary.

## II. THEORETICAL FRAMEWORK

### A. The potential model

The potential model is an effective approach to study the two-body bound state problem. For the  $H\bar{S} + h.c.$  system, the scattering between the charmed and anti-charmed meson occurs via exchanging the light pseudoscalar, scalar and vector mesons, which play the role of providing long-distant, intermediate-distance and short-distance forces. At the

---

‡ Corresponding author

\*Electronic address: chenxl@pku.edu.cn

†Electronic address: zhushl@pku.edu.cn

§Electronic address: xiangliu@lzu.edu.cn

hadron level, there exist two types of diagrams in the scattering of the charmed and anti-charmed mesons, i.e., the cross and direct diagrams as shown in Table III. The exchanged light mesons relevant to the four subsystems  $[PP_0^*]$ ,  $[PP_1]$ ,  $[P^*P_0^*]$  and  $[P^*P_1]$  are also presented in Table III. When writing out the scattering amplitude, the monopole form factor is introduced at every interaction vertex to compensate the off-shell effect of the exchanged light meson

$$\mathcal{F}(q) = \frac{\Lambda^2 - m^2}{\Lambda^2 - q^2}, \quad (1)$$

where the phenomenological cutoff parameter  $\Lambda$  is about 1 GeV.  $q$  and  $m$  denote the four-momentum and the mass of the exchanged meson.

<i>H</i> doublet						
$J^P$	charmed-up(down) meson				charmed-strange meson	
	charged mass (MeV)	neutral mass (MeV)			charged mass (MeV)	
$0^-$	$D^\pm$	1869.3	$D^0$	1864.5	$D_s^\pm$	1968.2
$1^-$	$D^{*\pm}$	2010.0	$D^{*0}$	2006.7	$D_s^{*\pm}$	2112.0
$J^P$	bottom-up(down) meson				bottom-strange meson	
	charged mass (MeV)	neutral mass (MeV)			neutral mass (MeV)	
$0^-$	$B^\pm$	5279.1	$B^0$	5279.5	$B_s^0$	5365.1
$1^-$	$B^{*\pm}$	5325.1	$B^{*0}$	5325.1	$B_s^{*0}$	5412.0
<i>S</i> doublet						
$J^P$	charmed-up(down) meson				charmed-strange meson	
	charged mass (MeV)	neutral mass (MeV)			charged mass (MeV)	
$0^+$	$D_0^\pm$	2403	$D_0^0$	2352	$D_{s0}^\pm$	2317.3
$1^+$	$D_1^{\pm}$	-	$D_1^{\prime 0}$	2427	$D_{s1}^{\pm}$	2458
$J^P$	bottom-up(down) meson				bottom-strange meson	
	charged mass (MeV)	neutral mass (MeV)			neutral mass (MeV)	
$0^+$	$B_0^\pm$	-	$B_0^0$	-	$B_{s0}^0$	-
$1^+$	$B_1^{\pm}$	-	$B_1^{\prime 0}$	-	$B_{s1}^0$	-

TABLE I: The masses of the heavy mesons in the *H* and *S* doublets [22].

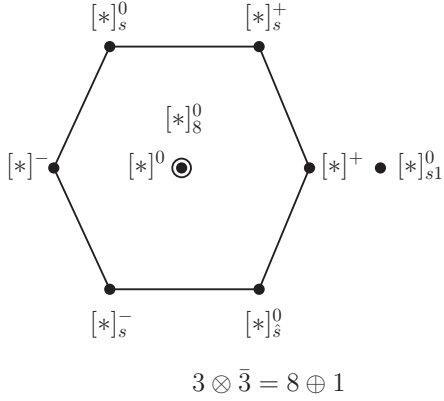
According to the effective Lagrangian describing the interaction between the light and charmed mesons, one can write down the scattering amplitude between the charmed and anti-charmed mesons. Such a system can be described as

$$|J, J_Z\rangle = \sum_{\lambda_1, \lambda_2} \langle J_1, \lambda_1; J_2, \lambda_2 | J, J_Z \rangle |p_1, p_2\rangle, \quad (2)$$

where  $J$  and  $J_i$  ( $i = 1, 2$ ) denote the angular momentum of the system and the components. The scattering amplitude  $i\mathcal{M}(J, J_Z)$  is related to the interaction potential in the momentum space in terms of the Breit approximation

$$\mathcal{V}(\mathbf{q}) = -\frac{1}{\sqrt{\prod_i 2m_i \prod_f 2m_f}} \mathcal{M}(J, J_Z). \quad (3)$$

Here,  $m_i$  and  $m_j$  denote the masses of the initial and final states respectively. The potential in the coordinate space  $\mathcal{V}(\mathbf{r})$  is obtained after Fourier transformation.



(a) $[PP_0^*]$ system		(b) $[PP_1']$ system	
States	Wave function	States	Wave function
$[PP_0^*]^+$	$\frac{1}{\sqrt{2}}[D^+\bar{D}_0^0 + c\bar{D}^0D_0^+]$	$[PP_1']^+$	$\frac{1}{\sqrt{2}}[D^+\bar{D}_1'^0 + c\bar{D}^0D_1'^+]$
$[PP_0^*]^0$	$\frac{1}{2}[(D^0\bar{D}_0^0 + c\bar{D}^0D_0^0)$ $-(D^+D_0^- + cD^-D_0^+)]$	$[PP_1']^0$	$\frac{1}{2}[(D^0\bar{D}_1'^0 + c\bar{D}^0D_1'^0)$ $-(D^+D_0^- + cD^-D_0^+)]$
$[PP_0^*]^-$	$\frac{1}{\sqrt{2}}[D^-\bar{D}_0^0 + c\bar{D}^0D_0^-]$	$[PP_1']^-$	$\frac{1}{\sqrt{2}}[D^-\bar{D}_1'^0 + c\bar{D}^0D_1'^-]$
$[PP_0^*]_s^+$	$\frac{1}{\sqrt{2}}[D_s^+\bar{D}_0^0 + c\bar{D}^0D_{s0}^+]$	$[PP_1']_s^+$	$\frac{1}{\sqrt{2}}[D_s^+\bar{D}_1'^0 + c\bar{D}^0D_{s1}^+]$
$[PP_0^*]_s^0$	$\frac{1}{\sqrt{2}}[D_s^+D_0^- + cD^-D_{s0}^+]$	$[PP_1']_s^0$	$\frac{1}{\sqrt{2}}[D_s^+D_1'^- + cD^-D_{s1}^+]$
$[PP_0^*]_s^-$	$\frac{1}{\sqrt{2}}[D_s^-\bar{D}_0^0 + c\bar{D}^0D_{s0}^-]$	$[PP_1']_s^-$	$\frac{1}{\sqrt{2}}[D_s^-\bar{D}_1'^0 + c\bar{D}^0D_{s1}^-]$
$[PP_0^*]_s^0$	$\frac{1}{\sqrt{2}}[D^+D_{s0}^- + cD_s^-D_0^+]$	$[PP_1']_s^0$	$\frac{1}{\sqrt{2}}[D^+D_{s1}^- + cD_s^-D_1'^+]$
$[PP_0^*]_s^0$	$\frac{1}{2}[(D^0\bar{D}_0^0 + c\bar{D}^0D_0^0)$ $+(D^+D_0^- + cD^-D_0^+)]$	$[PP_1']_s^0$	$\frac{1}{2}[(D^0\bar{D}_1'^0 + c\bar{D}^0D_1'^0)$ $+(D^+D_1'^- + cD^-D_1'^+)]$
$[PP_0^*]_{s1}^0$	$\frac{1}{\sqrt{2}}[D_s^+D_{s0}^- + cD_s^-D_{s0}^+]$	$[PP_1']_{s1}^0$	$\frac{1}{\sqrt{2}}[D_s^+D_{s1}^- + cD_s^-D_{s1}^+]$
(c) $[P^*P_0^*]$ system		(d) $[P^*P_1']$ system	
States	Wave function	States	Wave function
$[P^*P_0^*]^+$	$\frac{1}{\sqrt{2}}[D^{*+}\bar{D}_0^0 + c\bar{D}^{*0}D_0^+]$	$[P^*P_1']^+$	$\frac{1}{\sqrt{2}}[D^{*+}\bar{D}_1'^0 + c\bar{D}^{*0}D_1'^+]$
$[P^*P_0^*]^0$	$\frac{1}{2}[(D^{*0}\bar{D}_0^0 + c\bar{D}^{*0}D_0^0)$ $-(D^{*+}D_0^- + cD^{*-}D_0^+)]$	$[P^*P_1']^0$	$\frac{1}{2}[(D^{*0}\bar{D}_1'^0 + c\bar{D}^{*0}D_1'^0)$ $-(D^{*+}D_0^- + cD^{*-}D_0^+)]$
$[P^*P_0^*]^-$	$\frac{1}{\sqrt{2}}[D^{*-}\bar{D}_0^0 + c\bar{D}^{*0}D_0^-]$	$[P^*P_1']^-$	$\frac{1}{\sqrt{2}}[D^{*-}\bar{D}_1'^0 + c\bar{D}^{*0}D_1'^-]$
$[P^*P_0^*]_s^+$	$\frac{1}{\sqrt{2}}[D_s^{*+}\bar{D}_0^0 + c\bar{D}^{*0}D_{s0}^+]$	$[P^*P_1']_s^+$	$\frac{1}{\sqrt{2}}[D_s^{*+}\bar{D}_1'^0 + c\bar{D}^{*0}D_{s1}^+]$
$[P^*P_0^*]_s^0$	$\frac{1}{\sqrt{2}}[D_s^{*+}D_0^- + cD^{*-}D_{s0}^+]$	$[P^*P_1']_s^0$	$\frac{1}{\sqrt{2}}[D_s^{*+}D_1'^- + cD^{*-}D_{s1}^+]$
$[P^*P_0^*]_s^-$	$\frac{1}{\sqrt{2}}[D_s^{*-}\bar{D}_0^0 + c\bar{D}^{*0}D_{s0}^-]$	$[P^*P_1']_s^-$	$\frac{1}{\sqrt{2}}[D_s^{*-}\bar{D}_1'^0 + c\bar{D}^{*0}D_{s1}^-]$
$[P^*P_0^*]_s^0$	$\frac{1}{\sqrt{2}}[D^{*+}D_{s0}^- + cD_s^{*-}D_0^+]$	$[P^*P_1']_s^0$	$\frac{1}{\sqrt{2}}[D^{*+}D_{s1}^- + cD_s^{*-}D_1'^+]$
$[P^*P_0^*]_s^0$	$\frac{1}{2}[(D^{*0}\bar{D}_0^0 + c\bar{D}^{*0}D_0^0)$ $+(D^{*+}D_0^- + cD^{*-}D_0^+)]$	$[P^*P_1']_s^0$	$\frac{1}{2}[(D^{*0}\bar{D}_1'^0 + c\bar{D}^{*0}D_1'^0)$ $+(D^{*+}D_1'^- + cD^{*-}D_1'^+)]$
$[P^*P_0^*]_{s1}^0$	$\frac{1}{\sqrt{2}}[D_s^{*+}D_{s0}^- + cD_s^{*-}D_{s0}^+]$	$[P^*P_1']_{s1}^0$	$\frac{1}{\sqrt{2}}[D_s^{*+}D_{s1}^- + cD_s^{*-}D_{s1}^+]$

TABLE II: The flavor wave functions of the  $[PP_0^*]$ ,  $[PP_1']$ ,  $[P^*P_0^*]$  and  $[P^*P_1']$  systems. We use  $[\dots]_b^a$  to name the different states, where the superscript  $a$  denotes the charge of the state and subscript  $b$  is introduced to distinguish the different states in a subsystem.

## B. The effective Lagrangian

The effective Lagrangian describing the interaction between the light and heavy flavor mesons is constructed with the help of the chiral symmetry and heavy quark symmetry [23]

$$\begin{aligned}
\mathcal{L} = & igTr[H_b\gamma_\mu\mathcal{A}_{ba}^\mu\gamma_5\bar{H}_a] + ig'Tr[S_b\gamma_\mu\mathcal{A}_{ba}^\mu\gamma_5\bar{S}_a] + \{ihTr[S_b\gamma_\mu\mathcal{A}_{ba}^\mu\gamma_5\bar{H}_a] + h.c.\} \\
& + i\beta Tr[H_b v^\mu(\mathcal{V}_\mu - \rho_\mu)_{ba}\bar{H}_a] + i\lambda Tr[H_b\sigma^{\mu\nu}F_{\mu\nu}(\rho)_{ba}\bar{H}_a] \\
& + i\beta' Tr[S_b v^\mu(\mathcal{V}_\mu - \rho_\mu)_{ba}\bar{S}_a] + i\lambda' Tr[S_b\sigma^{\mu\nu}F_{\mu\nu}(\rho)_{ba}\bar{S}_a] \\
& + \{i\zeta Tr[H_b\gamma^\mu(\mathcal{V}_\mu - \rho_\mu)_{ba}\bar{S}_a] + i\mu Tr[H_b\sigma^{\mu\nu}F_{\mu\nu}(\rho)_{ba}\bar{S}_a] + h.c.\} \\
& + g_\sigma Tr[H_a\sigma\bar{H}_a] + g'_\sigma Tr[S_a\sigma\bar{S}_a] + \left\{\frac{h_\sigma}{f_\pi}Tr[S_a(\partial_\mu\sigma)\gamma^\mu\bar{H}_a] + h.c.\right\}.
\end{aligned} \tag{4}$$

The  $H$  and  $S$  fields, which correspond to the  $(0^-, 1^-)$  and  $(0^+, 1^+)$  doublets are defined respectively

$$\begin{aligned}
H_a &= \frac{1+\not{v}}{2}[P_{a\mu}^*\gamma^\mu + iP_a\gamma_5], \\
\bar{H}_b &= \gamma^0 H^\dagger \gamma^0 = [P_{a\mu}^{\dagger}\gamma^\mu + iP_a^\dagger\gamma_5]\frac{1+\not{v}}{2}, \\
S_a &= \frac{1+\not{v}}{2}[P'_{1a}\gamma^\mu\gamma_5 - P_{0a}^*], \\
\bar{S}_a &= \gamma^0 S^\dagger \gamma^0 = [P'_{1a}\gamma^\mu\gamma_5 - P_{0a}^{*\dagger}]\frac{1+\not{v}}{2},
\end{aligned} \tag{5}$$

where  $v = (1, 0, 0, 0)$ . Here, the annihilation operations  $P$ ,  $P_\mu^*$ ,  $P_0^*$ ,  $P'_{1\mu}$  are of dimension 3/2 and satisfy the normalization relations

$$\begin{aligned}
\langle 0|P|Q\bar{q}(0^-)\rangle &= \sqrt{M_H}, & \langle 0|P_\mu^*|Q\bar{q}(0^-)\rangle &= \epsilon_\mu\sqrt{M_H}, \\
\langle 0|P_0^*|Q\bar{q}(0^+)\rangle &= \sqrt{M_S}, & \langle 0|P'_{1\mu}|Q\bar{q}(1^+)\rangle &= \epsilon_\mu\sqrt{M_S}.
\end{aligned}$$

In Eq. (4), the expansion of the axial vector gives

$$\mathcal{A}_\mu = \frac{1}{2}(\xi^\dagger\partial_\mu\xi - \xi\partial_\mu\xi^\dagger) = \frac{i}{f_\pi}\partial_\mu\mathcal{M} + \dots \tag{6}$$

with  $\xi = \exp(i\mathbb{P}/f_\pi)$  and  $f_\pi = 132$  MeV.  $\rho_{ba}^\mu = ig_v\nabla_{ba}^\mu/\sqrt{2}$  and  $F_{\mu\nu}(\rho) = \partial_\mu\rho_\nu - \partial_\nu\rho_\mu + [\rho_\mu, \rho_\nu]$ . The octet pseudoscalar and nonet vector meson matrices read as

$$\mathbb{P} = \begin{pmatrix} \frac{\pi^0}{\sqrt{2}} + \frac{\eta}{\sqrt{6}} & \pi^+ & K^+ \\ \pi^- & -\frac{\pi^0}{\sqrt{2}} + \frac{\eta}{\sqrt{6}} & K^0 \\ K^- & \bar{K}^0 & -\frac{2\eta}{\sqrt{6}} \end{pmatrix}, \quad \mathbb{V} = \begin{pmatrix} \frac{\rho^0}{\sqrt{2}} + \frac{\omega}{\sqrt{2}} & \rho^+ & K^{*+} \\ \rho^- & -\frac{\rho^0}{\sqrt{2}} + \frac{\omega}{\sqrt{2}} & K^{*0} \\ K^{*-} & \bar{K}^{*0} & \phi \end{pmatrix}. \tag{7}$$

After expanding Eq. (4), the effective Lagrangian of the pseudoscalar mesons with heavy flavor mesons reads

$$\mathcal{L}_{\mathcal{D}^*\mathcal{D}^*\mathbb{P}} = \frac{g}{f_\pi}\varepsilon_{\alpha\mu\beta\nu}(2iv^\alpha P_b^{*\mu}P_a^{*\nu\dagger})\partial^\beta\mathbb{P}_{ba}, \tag{8}$$

$$\mathcal{L}_{\mathcal{D}^*\mathcal{D}\mathbb{P}} = i\frac{2g}{f_\pi}(P_b P_{a\lambda}^{*\dagger} - P_{b\lambda}^* P_a^\dagger)\partial^\lambda\mathbb{P}_{ba}, \tag{9}$$

$$\mathcal{L}_{\mathcal{D}'_1\mathcal{D}'_1\mathbb{P}} = \frac{g'}{f_\pi}\varepsilon_{\alpha\mu\beta\nu}(2iv^\alpha)P'_{1b}{}^\mu P'_{1a}{}^{\nu\dagger}\partial^\beta\mathbb{P}_{ba}, \tag{10}$$

$$\mathcal{L}_{\mathcal{D}\mathcal{D}_0^*\mathbb{P}} = \frac{h}{f_\pi}(2iv_\mu)(P_{0b}^*P_a^\dagger - P_b P_{0a}^{*\dagger})\partial^\mu\mathbb{P}_{ba}, \tag{11}$$

$$\mathcal{L}_{\mathcal{D}^*\mathcal{D}'_1\mathbb{P}} = i\frac{h}{f_\pi}(P'_{1b} \cdot P_a^{*\dagger} + P_b^* \cdot P'_{1a}{}^\dagger)(2iv) \cdot \partial\mathbb{P}_{ba}. \tag{12}$$

	Direct diagram			Crossed diagram		
Subsystems	Pseudoscalar	Vector	Scalar	Pseudoscalar	Vector	Scalar
	( $\mathbb{P}$ )	( $\mathbb{V}$ )	( $\mathbb{S}$ )	( $\mathbb{P}$ )	( $\mathbb{V}$ )	( $\mathbb{S}$ )
$[PP_0^*]$		✓	✓	✓		
$[PP_1']$		✓	✓		✓	✓
$[P^*P_0^*]$		✓	✓		✓	✓
$[P^*P_1']$	✓	✓	✓	✓	✓	✓

TABLE III: The direct and crossed scattering diagrams with the exchanged light mesons for the  $H\bar{S} + h.c.$  system .

The effective Lagrangian of the vector mesons with heavy flavor mesons reads

$$\mathcal{L}_{\mathcal{D}\mathcal{D}\mathbb{V}} = i\frac{\beta g_V}{\sqrt{2}}P_b P_a^\dagger (2iv_\mu)\mathbb{V}_{ba}^\mu, \quad (13)$$

$$\mathcal{L}_{\mathcal{D}^*\mathcal{D}\mathbb{V}} = -2\frac{\lambda g_V}{\sqrt{2}}(2iv^\lambda)\varepsilon_{\lambda\alpha\beta\mu}(P_b P_a^{*\mu\dagger} - P_b^{*\mu} P_a^\dagger)(\partial^\alpha\mathbb{V}^\beta)_{ba}, \quad (14)$$

$$\mathcal{L}_{\mathcal{D}^*\mathcal{D}^*\mathbb{V}} = -i\frac{\beta g_V}{\sqrt{2}}P_b^* \cdot P_a^{\dagger\dagger}(2iv \cdot \mathbb{V}_{ba}) - i4\frac{\lambda g_V}{\sqrt{2}}P_b^{*\mu} P_a^{*\nu\dagger}(\partial_\mu\mathbb{V}_\nu - \partial_\nu\mathbb{V}_\mu)_{ba}, \quad (15)$$

$$\mathcal{L}_{\mathcal{D}_0^*\mathcal{D}_0^*\mathbb{V}} = -i\frac{\beta' g_V}{\sqrt{2}}P_{0b}^* P_{0a}^{\dagger\dagger}(2iv \cdot \mathbb{V}_{ba}), \quad (16)$$

$$\mathcal{L}_{\mathcal{D}_0^*\mathcal{D}^*\mathbb{V}} = -2\frac{\zeta g_V}{\sqrt{2}}(P_b^{*\mu} P_{0a}^{\dagger\dagger} + P_{0b}^* P_a^{*\mu\dagger})\mathbb{V}_{\mu ba} - 2\frac{\varpi g_V}{\sqrt{2}}(2iv^\alpha)(P_b^{*\beta} P_{0a}^{\dagger\dagger} - P_{0b}^* P_a^{*\beta\dagger})(\partial_\alpha\mathbb{V}_\beta - \partial_\beta\mathbb{V}_\alpha)_{ba}, \quad (17)$$

$$\mathcal{L}_{\mathcal{D}'_1\mathcal{D}'_1\mathbb{V}} = i\frac{\beta' g_V}{\sqrt{2}}P'_{1b} \cdot P'_{1a}{}^\dagger(2iv \cdot \mathbb{V}_{ba}) + i4\frac{\lambda' g_V}{\sqrt{2}}P'_{1b\mu} P'_{1a\nu}{}^\dagger(\partial^\mu\mathbb{V}^\nu - \partial^\nu\mathbb{V}^\mu)_{ba}, \quad (18)$$

$$\mathcal{L}_{\mathcal{D}'_1\mathcal{D}\mathbb{V}} = i2\frac{\zeta g_V}{\sqrt{2}}(P_b P'_{1a}{}^{\mu\dagger} - P'_{1b}{}^\mu P_a^\dagger)\mathbb{V}_{\mu ba} + i2\frac{\varpi g_V}{\sqrt{2}}(2iv^\alpha)(P_b P'_{1a}{}^{\beta\dagger} + P'_{1b}{}^\beta P_a^\dagger)(\partial_\alpha\mathbb{V}_\beta - \partial_\beta\mathbb{V}_\alpha)_{ba}, \quad (19)$$

$$\mathcal{L}_{\mathcal{D}'_1\mathcal{D}^*\mathbb{V}} = \frac{\zeta g_V}{\sqrt{2}}(2iv^\lambda)\varepsilon_{\lambda\nu\mu\delta}(P_b^{*\nu} P'_{1a}{}^{\delta\dagger} - P'_{1b}{}^\delta P_a^{*\nu\dagger})\mathbb{V}_{ba}^\mu + 2\frac{\varpi g_V}{\sqrt{2}}\varepsilon_{\nu\alpha\beta\mu}(P_b^{*\nu} P'_{1a}{}^{\mu\dagger} + P'_{1b}{}^\mu P_a^{*\nu\dagger})(\partial^\alpha\mathbb{V}^\beta - \partial^\beta\mathbb{V}^\alpha)_{ba}, \quad (20)$$

$$\mathcal{L}_{\mathcal{D}\mathcal{D}'_1\mathbb{V}} = i2\frac{\zeta g_V}{\sqrt{2}}(P_b P'_{1a}{}^{\mu\dagger} - P_a^\dagger P'_{1b}{}^\mu)\mathbb{V}_{\mu ba} - i2\frac{\varpi g_V}{\sqrt{2}}(2iv^\beta)(P_b P'_{1a}{}^{\alpha\dagger} + P'_{1b}{}^\alpha P_a^\dagger)(\partial_\alpha\mathbb{V}_\beta - \partial_\beta\mathbb{V}_\alpha)_{ba}, \quad (21)$$

$$\mathcal{L}_{\mathcal{D}'_1\mathcal{D}_0^*\mathbb{V}} = i2\frac{\lambda' g_V}{\sqrt{2}}(2iv^\lambda)\varepsilon_{\lambda\alpha\beta\mu}(P_{0b}^* P'_{1a}{}^{\mu\dagger} + P'_{1b}{}^\mu P_{0a}^{\dagger\dagger})(\partial^\alpha\mathbb{V}^\beta)_{ba}. \quad (22)$$

The effective Lagrangian of the  $\sigma$  meson interacting with heavy flavor mesons reads

$$\mathcal{L}_{\mathcal{D}\mathcal{D}\sigma} = -2g_\sigma\sigma P_b P_b^\dagger, \quad (23)$$

$$\mathcal{L}_{\mathcal{D}^*\mathcal{D}^*\sigma} = 2g_\sigma\sigma P_b^* \cdot P_b^{*\dagger}, \quad (24)$$

$$\mathcal{L}_{\mathcal{D}_0^*\mathcal{D}_0^*\sigma} = 2g'_\sigma\sigma P_{0b}^* P_{0b}^{\dagger\dagger}, \quad (25)$$

$$\mathcal{L}_{\mathcal{D}'_1\mathcal{D}'_1\sigma} = -2g'_\sigma\sigma P'_{1b} \cdot P'_{1b}{}^\dagger, \quad (26)$$

$$\mathcal{L}_{\mathcal{D}\mathcal{D}'_1\sigma} = -i\frac{2h_\sigma}{f_\pi}(P'_{1b\mu}P'_b{}^\dagger - P_bP'_{1b\mu}{}^\dagger)\partial^\mu\sigma, \quad (27)$$

$$\mathcal{L}_{\mathcal{D}^*\mathcal{D}'_0\sigma} = -\frac{2h_\sigma}{f_\pi}(P_{0b}^*P_b^{*\lambda\dagger} + P_b^{*\lambda}P_{0b}^{*\dagger})\partial^\lambda\sigma, \quad (28)$$

$$\mathcal{L}_{\mathcal{D}^*\mathcal{D}'_1\sigma} = i\frac{2h_\sigma}{f_\pi}v^\alpha\varepsilon_{\alpha\mu\lambda\nu}(P_{1a}^{\prime\mu}P_a^{*\nu\dagger} - P_a^{*\nu}P_{1a}^{\prime\mu\dagger})\partial^\lambda\sigma. \quad (29)$$

The values of the parameters  $g^{(\prime)}$ ,  $\beta^{(\prime)}$ ,  $\lambda^{(\prime)}$ ,  $h$ ,  $\varpi$ ,  $\zeta$ ,  $g_\sigma^{(\prime)}$  and  $h_\sigma$  are discussed in Refs. [23, 24].

### C. The effective potential of the $H\bar{S} + h.c.$ system

We list the effective potentials of the states in the  $H\bar{S} + h.c.$  system in Table IV. Here  $V_i^j$ ,  $Q_i^j$ ,  $W_i^j$  and  $O_i^j$  are the sub-potentials corresponding to the subsystems  $[PP_0^*]$ ,  $[PP'_1]$ ,  $[P^*P_0^*]$  and  $[P^*P'_1]$  respectively. The parameters in front of the sub-potentials in Table IV are from the coefficients in the octet pseudoscalar and nonet vector meson matrices.

For the  $[PP_0^*]$  subsystem, the sub-potentials are

$$V_{\mathbb{V}}^{Direct}(r) = -\frac{1}{2}\beta\beta'g_V^2Y(\Lambda, q_0, m_{\mathbb{V}}, r), \quad (30)$$

$$V_{\sigma}^{Direct}(r) = -g_\sigma g'_\sigma Y(\Lambda, q_0, m_\sigma, r), \quad (31)$$

$$V_{\mathbb{P}}^{Cross}(r) = \frac{h^2q_0'^2}{f_\pi^2}Y(\Lambda, q'_0, m_{\mathbb{P}}, r). \quad (32)$$

For the  $[PP'_1]$  subsystem, the sub-potentials are

$$Q_{\mathbb{V}}^{Direct}(r) = -\frac{1}{2}\beta\beta'g_V^2Y(\Lambda, q_0, m_{\mathbb{V}}, r), \quad (33)$$

$$Q_{\sigma}^{Direct}(r) = -g_\sigma g'_\sigma Y(\Lambda, q_0, m_\sigma, r), \quad (34)$$

$$\begin{aligned} Q_{\mathbb{V}}^{Cross}(r) &= -\frac{g_V^2}{4}(2\zeta^2 - 8\zeta\varpi q'_0 + 8\varpi^2 q_0'^2)Y(\Lambda, q'_0, m_{\mathbb{V}}, r) \\ &\quad + \frac{g_V^2}{12}(8\mu^2 - \frac{2\zeta^2}{m_V^2})Z(\Lambda, q'_0, m_{\mathbb{V}}, r), \end{aligned} \quad (35)$$

$$Q_{\sigma}^{Cross}(r) = -\frac{h_\sigma^2}{3f_\pi^2}Z(\Lambda, q'_0, m_\sigma, r). \quad (36)$$

The sub-potentials relevant to the  $[P^*P_0^*]$  subsystem are

$$W_{\mathbb{V}}^{Direct}(r) = -\frac{1}{2}\beta\beta'g_V^2Y(\Lambda, q_0, m_{\mathbb{V}}, r), \quad (37)$$

$$W_{\sigma}^{Direct}(r) = -g_\sigma g'_\sigma Y(\Lambda, q_0, m_\sigma, r), \quad (38)$$

$$\begin{aligned} W_{\mathbb{V}}^{Cross}(r) &= \frac{1}{4}g_V^2(2\zeta^2 - 8\zeta\varpi q'_0 + 8\varpi^2 q_0'^2)Y(\Lambda, q'_0, m_{\mathbb{V}}, r) \\ &\quad - \frac{1}{12}g_V^2(8\mu^2 - \frac{2\zeta^2}{m_{\mathbb{V}}^2})Z(\Lambda, q'_0, m_{\mathbb{V}}, r), \end{aligned} \quad (39)$$

$$W_{\sigma}^{Cross}(r) = \frac{h_\sigma^2}{f_\pi^2}\frac{1}{3}Z(\Lambda, q'_0, m_\sigma, r). \quad (40)$$

States	Effective potential
$[PP_0^*]^{\pm,0}$	$[-\frac{1}{2}V_\rho^{Direct}(r) + \frac{1}{2}V_\omega^{Direct}(r) + V_\sigma^{Direct}(r)] + c[-\frac{1}{2}V_\pi^{Cross}(r) + \frac{1}{6}V_\eta^{Cross}(r)]$
$[PP_1']^{\pm,0}$	$[-\frac{1}{2}Q_\rho^{Direct}(r) + \frac{1}{2}Q_\omega^{Direct}(r) + Q_\sigma^{Direct}(r)] + c[-\frac{1}{2}Q_\rho^{Cross}(r) + \frac{1}{2}Q_\omega^{Cross}(r) + Q_\sigma^{Cross}(r)]$
$[P^*P_0^*]^{\pm,0}$	$[-\frac{1}{2}W_\rho^{Direct}(r) + \frac{1}{2}W_\omega^{Direct}(r) + W_\sigma^{Direct}(\sigma)] + c[-\frac{1}{2}W_\rho^{Cross}(r) + \frac{1}{2}W_\omega^{Cross}(r) + W_\sigma^{Cross}(r)]$
$[P^*P_1']^{\pm,0}$	$[-\frac{1}{2}O_\rho^{Direct}(r) + \frac{1}{2}O_\omega^{Direct}(r) - \frac{1}{2}O_\pi^{Direct}(r) + \frac{1}{6}O_\eta^{Direct}(r) + O_\sigma^{Direct}(r)]$ $+c[-\frac{1}{2}O_\pi^{Cross}(r) + \frac{1}{6}O_\eta^{Cross}(r) - \frac{1}{2}O_\rho^{Cross}(r) + \frac{1}{2}O_\omega^{Cross}(r) + O_\sigma^{Cross}(r)]$
$[PP_0^*]_s^{\pm,0}, [PP_0^*]_s^0$	$c[-\frac{1}{3}V_\eta^{Cross}(r)]$
$[PP_1']_s^{\pm,0}, [PP_1']_s^0$	0
$[P^*P_0^*]_s^{\pm,0}, [P^*P_0^*]_s^0$	0
$[P^*P_1']_s^{\pm,0}, [P^*P_1']_s^0$	$[-\frac{1}{3}O_\eta^{Direct}(r)] + c[-\frac{1}{3}O_\eta^{Cross}(r)]$
$[PP_0^*]_{s1}^0$	$[V_\phi^{Direct}(r)] + c[\frac{2}{3}V_\eta^{Cross}(r)]$
$[PP_1']_{s1}^0$	$[Q_\phi^{Direct}(r)] + c[Q_\phi^{Cross}(r)]$
$[P^*P_0^*]_{s1}^0$	$[W_\phi^{Direct}(r)] + c[W_\phi^{Cross}(r)]$
$[P^*P_1']_{s1}^0$	$[O_\phi^{Direct}(r) + \frac{2}{3}O_\eta^{Direct}(r)] + c[O_\phi^{Cross}(r) + \frac{2}{3}O_\eta^{Cross}(r)]$
$[PP_0^*]_8^0$	$[\frac{3}{2}V_\rho^{Direct}(r) + \frac{1}{2}V_\omega^{Direct}(r) + V_\sigma^{Direct}(r)] + c[\frac{3}{2}V_\pi^{Cross}(r) + \frac{1}{6}V_\eta^{Cross}(r)]$
$[PP_1']_8^0$	$[\frac{3}{2}Q_\rho^{Direct}(r) + \frac{1}{2}Q_\omega^{Direct}(r) + Q_\sigma^{Direct}(r)] + c[\frac{3}{2}Q_\rho^{Cross}(r) + \frac{1}{2}Q_\omega^{Cross}(r) + Q_\sigma^{Cross}(r)]$
$[P^*P_0^*]_8^0$	$[\frac{3}{2}W_\rho^{Direct}(r) + \frac{1}{2}W_\omega^{Direct}(r) + W_\sigma^{Direct}(r)] + c[\frac{3}{2}W_\rho^{Cross}(r) + \frac{1}{2}W_\omega^{Cross}(r) + W_\sigma^{Cross}(r)]$
$[P^*P_1']_8^0$	$[\frac{3}{2}O_\rho^{Direct}(r) + \frac{1}{2}O_\omega^{Direct}(r) + \frac{3}{2}O_\pi^{Direct}(r) + \frac{1}{6}O_\eta^{Direct}(r) + O_\sigma^{Direct}(r)]$ $+c[\frac{3}{2}O_\pi^{Cross}(r) + \frac{1}{6}O_\eta^{Cross}(r) + \frac{3}{2}O_\rho^{Cross}(r) + \frac{1}{2}O_\omega^{Cross}(r) + O_\sigma^{Cross}(r)]$

TABLE IV: The total effective potentials of the states in the subsystems  $[PP_0^*]$ ,  $[PP_1']$ ,  $[P^*P_0^*]$  and  $[P^*P_1']$ .

For the  $[P^*\bar{P}'_1]$  subsystem, the relevant potentials are

$$O_{\mathbb{V}}^{Direct}(r) = -\frac{1}{2}g_{\mathbb{V}}^2\beta\beta' C[J]Y(\Lambda, q_0, m_{\mathbb{V}}, r) - 2g_{\mathbb{V}}^2\lambda\lambda' B[J]Z(\Lambda, q_0, m_{\mathbb{V}}, r), \quad (41)$$

$$O_{\mathbb{P}}^{Direct}(r) = -\frac{gg'}{f_\pi^2} A[J]Z(\Lambda, q_0, m_{\mathbb{V}}, r), \quad (42)$$

$$O_\sigma^{Direct}(r) = -g_\sigma g'_\sigma C[J]Y(\Lambda, q_0, m_{\mathbb{V}}, r), \quad (43)$$

$$O_{\mathbb{V}}^{Cross}(r) = \frac{1}{4}g_{\mathbb{V}}^2(2\zeta^2 - 8\zeta\varpi q'_0 + 8\varpi^2 q_0'^2) C[J]Y(\Lambda, q'_0, m_{\mathbb{V}}, r)$$

$$- \frac{1}{4}g_{\mathbb{V}}^2\left(\frac{2\zeta^2}{m_{\mathbb{V}}^2} - 8\mu^2\right) A[J]Z(\Lambda, q_0, m_{\mathbb{V}}, r), \quad (44)$$

$$O_{\mathbb{P}}^{Cross}(r) = -\frac{h^2}{f_\pi^2} q_0'^2 C[J]Y(\Lambda, q'_0, m_{\mathbb{P}}, r), \quad (45)$$

$$O_\sigma^{Cross}(r) = -\frac{h_\sigma^2}{f_\pi^2} A[J]Z(\Lambda, q'_0, m_\sigma, r) \quad (46)$$

with the coefficients  $A[J]$ ,  $B[J]$  and  $C[J]$

	J=0	J=1	J=2
A[J]	2/3	1/3	-1/3
B[J]	4/3	2/3	-2/3
C[J]	1	1	1

(47)

In the above expressions, the functions  $Y(\Lambda, \kappa, m, r)$  and  $Z(\Lambda, \kappa, m, r)$  are defined as

$$\begin{aligned}
 Y(\Lambda, \kappa, m, r) &= \int \frac{d^3q}{(2\pi)^3} e^{i\mathbf{q}\cdot\mathbf{r}} \frac{1}{\mathbf{q}^2 - \kappa^2 - m^2} \left( \frac{\Lambda^2 - m^2}{\Lambda^2 - \mathbf{q}^2 + \kappa^2} \right)^2 \\
 &= \begin{cases} \text{if } |\kappa| \leq m, & -\frac{1}{4\pi r} (e^{-\zeta_1 r} - e^{-\zeta_2 r}) + \frac{1}{8\pi} \left( \zeta_2 - \frac{\zeta_1^2}{\zeta_2} \right) e^{-\zeta_2 r} \\ \text{otherwise,} & -\frac{1}{4\pi r} (\cos(\zeta_1' r) - e^{-\zeta_2 r}) + \frac{1}{8\pi} \left( \zeta_2 + \frac{\zeta_1'^2}{\zeta_2} \right) e^{-\zeta_2 r} \end{cases}
 \end{aligned}
 \tag{48}$$

and

$$Z(\Lambda, \kappa, m, r) = -\frac{1}{r^2} \frac{\partial}{\partial r} \left( r^2 \frac{\partial}{\partial r} Y(\Lambda, \kappa, m, r) \right),
 \tag{49}$$

where  $\zeta_1 = \sqrt{m^2 - \kappa^2}$ ,  $\zeta_1' = \sqrt{\kappa^2 - m^2}$ , and  $\zeta_2 = \sqrt{\Lambda^2 - \kappa^2}$ . We take  $q_0 = 0$  and the mass differences  $q'_0$  as  $(m_{P_0} - m_P)$ ,  $(m_{P'_1} - m_P)$ ,  $(m_{P_0} - m_{P^*})$  and  $(m_{P'_1} - m_{P^*})$  corresponding to the  $[PP_0^*]$ ,  $[PP'_1]$ ,  $[P^*P_0]$  and  $[P^*P'_1]$  subsystems respectively.

### III. NUMERICAL RESULTS

In the following, we present the numerical results for the different systems. Throughout this work,  $\mu$  denotes the reduced mass of the corresponding system in all figures of the numerical results.

#### A. The $[PP_0^*]$ system

##### 1. $[PP_0^*]^{\pm,0}$

The total potentials of the  $[PP_0^*]^{\pm,0}$  system with  $c = \pm 1$  and the typical values of  $\Lambda$  are presented in Fig. 1. The comparison of the total potential with the partial potentials indicates that the  $\pi$  exchange plays the dominant role in the total effective potential of the  $[PP_0^*]^{\pm,0}$  system with  $c = \pm 1$ . Here we only illustrate the potential with  $\Lambda = 1$  GeV in Fig. 1 (b) and (d).

Since the one  $\pi$  exchange potential is dominant in the total potential of  $[PP_0^*]^{\pm,0}$ , it's enough to consider the one  $\pi$  exchange force only when we study the bound state solution of the  $[PP_0^*]^{\pm,0}$  system. The one  $\pi$  exchange potential is proportional to the coupling constant  $h$ . Thus, we try to solve the schrödinger equation with the obtained one pion exchange potential under some typical values of  $h$ .

For the  $[PP_0^*]^{\pm,0}$  system with  $c = +1$ , we can find the bound state solutions numerically. As shown in Fig. 2, the binding energy  $E_0$  decreases when  $\Lambda$  becomes larger. One may further check the corresponding wave function to make sure whether the bound state solution is reasonable. An example is shown in Fig. 2 (a) with  $h \equiv -0.56$ . As  $\Lambda$  increases, the wave function oscillates at large distance. In other words, smaller  $\Lambda$  values such as  $\Lambda < 0.75$  GeV lead to the bound state wave function with less oscillating behavior. On the other hand, the reasonable range of  $\Lambda$  is sometimes assumed to be around 1 GeV.

Enhancing the coupling constant helps to form the bound state of  $[PP_0^*]^{\pm,0}$  system with  $c = +1$ . For example, there exist a very reasonable bound state solution with  $1.3h$  corresponding to a shallow binding energy, a reasonable  $\Lambda$  and wave function with good behavior as shown in Fig. 2 (b). If the coupling constant becomes even larger, the binding energy of the  $[PP_0^*]^{\pm,0}$  system with  $c = +1$  becomes deeper. As shown in Fig 2 (c) and (d), there only exist deeply bound states for the  $[PP_0^*]^{\pm,0}$  system ( $c = +1$ ) with  $2h$  and  $3h$ .

For the  $[PP_0^*]^{\pm,0}$  system with  $c = -1$ , we can not find the bound state solution with  $1h$ . With  $2h$  and  $\Lambda = 2.6 \sim 3$  GeV, the wave function of the  $[PP_0^*]^{\pm,0}$  system with  $c = -1$  becomes non-oscillating. When further increasing the coupling constant to  $3h$ , there exists a  $[PP_0^*]^{\pm,0}$  bound state with  $c = -1$  and  $\Lambda$  near 1 GeV. The numerical results of the  $[PP_0^*]^{\pm,0}$  system with  $c = -1$  are presented in Fig. 3.

## 2. $[PP_0^*]_s^{\pm,0}, [PP_0^*]_s^0$

The potential of  $[PP_0^*]_s^{\pm,0}, [PP_0^*]_s^0$  is shown in Fig. 4, where only the  $\eta$  meson exchange contributes. The effective potential is repulsive and attractive for  $c = +1$  and  $c = -1$  respectively. There does not exist any bound states with  $c = +1$ .

For the  $[PP_0^*]_s^{\pm,0}, [PP_0^*]_s^0$  system with  $c = -1$ , we can not find the bound state solution with  $h \equiv -0.56$ . We illustrate the numerical results with  $2h$  and  $3h$  in Fig. 5. There may exist a  $[PP_0^*]_s^{\pm,0}, [PP_0^*]_s^0$  bound state with  $c = -1$  if the coupling constant is around several  $h$ .

## 3. $[PP_0^*]_{s1}^0$

In Fig. 6, we plot the variation of the effective potential of the  $[PP_0^*]_{s1}^0$  system with  $r$  and different coupling constants and the cutoff parameter. The  $\eta$  and  $\phi$  meson exchange contributes to the total effective potential. The cutoff  $\Lambda$  should be larger than the mass of  $\phi$  meson. The total effective potentials with  $(c = +1, \beta\beta' < 0)$  and  $(c = -1, \beta\beta' < 0)$  are attractive while the effective potentials with  $(c = +1, \beta\beta' > 0)$  and  $(c = -1, \beta\beta' > 0)$  are repulsive. The comparison of the total potential with the  $\eta$  and  $\phi$  meson exchange potential is given in Fig. 6 (e) and (f) with  $\Lambda = 1.5$  GeV.

For the  $[PP_0^*]_{s1}^0$  system with  $c = -1$ , there does not exist a bound state not only for the case  $\beta\beta' > 0$  but also for  $\beta\beta' < 0$ . For the  $[PP_0^*]_{s1}^0$  system with  $c = +1$  and  $\beta\beta' > 0$ , a reasonable solution of bound state appears with  $3h$ . For the  $[PP_0^*]_{s1}^0$  system with  $c = +1$  and  $\beta\beta' < 0$ , there does not exist a bound state with  $1h$ . The bound state solution appears with  $2h$  and  $3h$ . The detailed numerical results of the  $[PP_0^*]_{s1}^0$  system with  $c = +1$  are shown in Fig. 7.

## 4. $[PP_0^*]_8^0$

The dependence of the total potential of the  $[PP_0^*]_8^0$  system on  $\Lambda$  is presented in Fig. 8. The total effective potential oscillates with  $r$ . The  $\pi, \eta, \sigma, \rho$  and  $\omega$  exchange contributes to the total exchange potential. With  $\Lambda = 1$  GeV, the corresponding  $\pi, \eta, \sigma, \rho$  and  $\omega$  exchange potentials for the  $[PP_0^*]_8^0$  systems with  $c = \pm 1$  are given in 8 (c) and (d). The  $\pi$  exchange potential is dominant. Therefore, we only consider the single pion exchange potential when we explore whether there exists the bound state solution of the  $[PP_0^*]_8^0$  system.

For the  $[PP_0^*]_8^0$  system with  $c = +1$ , there exists a bound state solution. The variation of the binding energy of  $[PP_0^*]_8^0$  with  $c = +1$  is shown in Fig. 9 with different values of the coupling constant. The wave functions is not reasonable when taking  $|h| = 0.56, 0.65, 0.7$ , which corresponds to the shallow binding energy of the  $[PP_0^*]_8^0$  system with  $c = +1$ . Increasing the coupling constant to  $2h$  leads to a bound state solution with a reasonable wave function.

The numerical result presented in Fig. 10 shows that there exists a  $[PP_0^*]_8^0$  bound state with  $c = -1$ .

## B. The $[PP'_1]$ system

### 1. $[PP'_1]^{\pm,0}$

The  $\sigma, \rho$  and  $\omega$  meson exchange contributes to the total effective potential of the  $[PP'_1]^{\pm,0}$  system. Since the  $\rho$  and  $\omega$  exchange potentials cancel each other, the  $\sigma$  meson exchange potential is dominant. We only need to consider the  $\sigma$  exchange potential in order to explore whether there exists a  $[PP'_1]^{\pm,0}$  bound state. In Fig. 11, the effective potential of the  $[PP'_1]^{\pm,0}$  system is presented. The  $\sigma$  exchange potential of the  $[PP'_1]^{\pm,0}$  system with  $c = +1$  is repulsive. There does not exist a  $[PP'_1]^{\pm,0}$  bound state with  $c = +1$ .

For the  $[PP'_1]^{\pm,0}$  system with  $c = -1$ , the  $\sigma$  exchange potential is attractive. Meanwhile, the cross diagram plays the dominant role. However, in the cases  $g_\sigma g'_\sigma > 0$  and  $g_\sigma g'_\sigma < 0$ , we can not find a bound state solution of the  $[PP'_1]^{\pm,0}$  system with  $c = -1$  and the coupling constants listed in the caption of Fig. 11 when scanning the range of cutoff  $\Lambda$ .

When taking  $2h_\sigma$ , we present the variation of the binding energy of the  $[PP_1']^{\pm,0}$  system with  $c = -1$  and the cutoff  $\Lambda$  in Fig. 12 in the cases  $g_\sigma g'_\sigma > 0$  and  $g_\sigma g'_\sigma < 0$ . However, the corresponding cutoff  $\Lambda$  is far larger than 1 GeV. Thus, we tend to conclude that there does not exist a  $[PP_1']^{\pm,0}$  bound state with  $c = -1$ .

2.  $[PP_1']_s^{\pm,0}, [PP_1']_s^0$

There does not exist the  $[PP_1']_s^{\pm,0}, [PP_1']_s^0$  bound state system since none of the meson exchange forces is allowed as indicated in Table IV.

3.  $[PP_1']_{s1}^0$

Here the effective potential of the  $[PP_1']_{s1}^0$  arises from the  $\phi$  meson exchange. There exist eight combinations of the parameters  $c, \beta\beta'$  and  $\zeta\varpi$ . With different parameters, the dependence of the effective potential of the  $[PP_1']_{s1}^0$  system with  $c = \pm 1$  on  $r$  is shown in Figs. 13-14.

When solving the Schrödinger equation, the cutoff  $\Lambda$  is expected to be larger than the mass of the  $\phi$  meson. We only find bound state solutions of  $[PP_1']_{s1}^0$  with  $c = -1, \beta\beta' < 0$  and  $\zeta\varpi < 0$ , which is shown in Fig. 15.

4.  $[PP_1']_8^0$

The  $\sigma, \rho, \omega$  exchange contributes to the total effective potential of  $[PP_1']_8^0$  system. In Fig. 16, the variation of the total effective potential of  $[PP_1']_8^0$  to  $r$  and different typical  $\Lambda$  values is given. The comparison of the total potential with the  $\sigma, \rho$  and  $\omega$  exchange potential is presented in Fig. 16 (c) and (d) with  $\Lambda = 1$  GeV.

Since the total potential is repulsive for the case of  $c = +1$ , we only explore whether there exists the bound state  $[PP_1']_8^0$  system with  $c = -1$ . The combinations of coupling constants  $g_\sigma g'_\sigma, \beta\beta'$  and  $\zeta\varpi$  are eight. However, we find the bound state solution of  $[PP_1']_8^0$  system with  $c = -1$  with six parameter combinations just listed in the caption of Fig. 17.

### C. The $[P^*P_0^*]$ system

1.  $[P^*P_0^*]^{\pm,0}$

The total effective potential of the  $[P^*P_0^*]^{\pm,0}$  system arises from the  $\sigma, \rho$  and  $\omega$  meson exchange. Since the  $\rho$  and  $\omega$  exchange potentials cancel each other, the  $\sigma$  exchange potential is dominant in the total effective potential of  $[P^*P_0^*]^{\pm,0}$ . We only consider the  $\omega$  exchange potential contribution to explore whether there exists a  $[P^*P_0^*]^{\pm,0}$  bound state. In Fig. 18, the effective potential of the  $[P^*P_0^*]^{\pm,0}$  system is presented.

The  $\sigma$  exchange potential of  $[PP_1']^{\pm,0}$  system with  $c = -1$  is repulsive. Thus there does not exist a  $[PP_1']^{\pm,0}$  bound state with  $c = -1$ .

For the  $[P^*P_0^*]^{\pm,0}$  system with  $c = +1$ , the  $\sigma$  exchange potential is attractive. Meanwhile, the cross diagram plays the dominant role to the  $\sigma$  exchange potential. However, in the  $g_\sigma g'_\sigma > 0$  and  $g_\sigma g'_\sigma < 0$  two cases, we can not find bound state solutions of the  $[P^*P_0^*]^{\pm,0}$  system with  $c = -1$  and the coupling constants listed in the caption of Fig. 18 when scanning the range of the cutoff  $\Lambda$ .

When taking  $2h_\sigma$ , we obtain the binding energy of the  $[P^*P_0^*]^{\pm,0}$  system with  $c = +1$  dependent on the cutoff  $\Lambda$  in Fig. 19 only in the  $g_\sigma g'_\sigma < 0$  case. However, the corresponding cutoff  $\Lambda$  is far larger than usual 1 GeV. Thus, the  $[P^*P_0^*]^{\pm,0}$  system with  $c = +1$  seems impossible to form the bound state.

2.  $[P^*P_0^*]_s^{\pm,0}, [P^*P_0^*]_s^0$

There does not exist the  $[P^*P_0^*]_s^{\pm,0}, [P^*P_0^*]_s^0$  bound state since no suitable meson exchange force is allowed as indicated in Table IV.

3.  $[P^*P_0]_{s1}^0$ 

Here, the effective potential of the  $[P^*P_0]_{s1}^0$  system results from the  $\phi$  meson exchange. There exist eight combinations of the parameters  $c$ ,  $\beta\beta'$  and  $\zeta\varpi$ . Under different parameter space, the dependence of the effective potential of  $[P^*P_0]_{s1}^0$  with  $c = \pm 1$  on  $r$  is listed in Figs. 20-21.

When solving the Schrödinger equation, the cutoff  $\Lambda$  should be larger than the mass of the  $\phi$  meson. There exists a bound state solution of the  $[P^*P_0]_{s1}^0$  system only with  $c = +1$ ,  $\beta\beta' < 0$  and  $\zeta\varpi < 0$ , which is shown in Fig. 22.

4.  $[P^*P_0]_8^0$ 

As indicated in Table IV, the behavior of the  $\rho$  meson exchange potential is similar to that of the  $\omega$  meson exchange potential. When exploring the  $[P^*P_0]_8^0$  system, we need to consider the  $\sigma$  exchange potential together with both the  $\rho$  and  $\omega$  meson exchanges. The relevant total and partial potentials are shown in Fig. 23.

Since the total potential of the  $[P^*P_0]_8^0$  system with  $c = -1$  is repulsive, there does not exist a  $[P^*P_0]_8^0$  bound state system with  $c = -1$ . In the following, we mainly focus on the  $[P^*P_0]_8^0$  system with  $c = +1$ , where the total effective potential is attractive. As shown in Fig. 24, there exists the bound state solution of the  $[P^*P_0]_8^0$  system with  $c = +1$ .

D. The  $[P^*P_1]$  system

In Refs. [13, 18, 19], the  $[P^*P_1]_{s1}^{\pm,0}$  and  $[P^*P_1]_8^0$  systems were studied. In this work we will discuss the rest two cases of the  $[P^*P_1]$  system, i.e.,  $[P^*P_1]_{s1}^{\pm,0}/[P^*P_1]_8^0$  and  $[P^*P_0]_{s1}^0$ .

1.  $[P^*P_1]_{s1}^{\pm,0}$ ,  $[P^*P_1]_8^0$ 

The effective potential of the  $[P^*P_1]_{s1}^{\pm,0}$ ,  $[P^*P_1]_8^0$  system arises from the  $\eta$  meson exchange only, which is plotted in Fig. 25 under several typical combinations of parameters.

When solving the the Schrödinger equation, we obtain the bound state solutions of the  $[D^*D_1]_{s1}^{\pm,0}$ ,  $[D^*D_1]_8^0$  system, which are listed in Fig. 26. The bound state solution of the  $[D^*D_1]_{s1}^{\pm,0}$ ,  $[D^*D_1]_8^0$  system appears when  $(c = +1, J = 0, gg' > 0)$ ,  $(c = +1, J = 0, gg' < 0)$ ,  $(c = +1, J = 1, gg' > 0)$ ,  $(c = +1, J = 1, gg' < 0)$ ,  $(c = +1, J = 2, gg' > 0)$  and  $(c = +1, J = 0, gg' < 0)$ . The above numerical results are obtained with  $3h$  while we can not find the bound state solution for  $1h$  and  $2h$ .

2.  $[P^*P_0]_{s1}^0$ 

The effective potential of the  $[P^*P_1]_{s1}^0$  system results from both the  $\eta$  and  $\phi$  meson exchanges as shown in Figs. 27 and 28.

There exist 96 combinations of the parameters  $c$ ,  $\beta\beta'$ ,  $gg'$ ,  $\lambda\lambda'$  and  $\zeta\varpi$ . When solving the Schrödinger equation, the cutoff  $\Lambda$  should be larger than the mass of the  $\phi$  meson. We only find bound state solutions of the  $[P^*P_1]_{s1}^0$  system under 20 combinations of  $c$ ,  $\beta\beta'$ ,  $gg'$ ,  $\lambda\lambda'$  and  $\zeta\varpi$ , which are shown in Figs. 29, 30 and 31 for  $J = 0, 1, 2$  cases respectively.

## IV. CONCLUSION

We have investigated the possible molecular states composed of a pair of heavy mesons in the  $H$  and  $S$  doublet. They are expected to be loosely bound states mainly via the long range pseudoscalar scalar meson exchange. We are interested in these shallow S-wave states with  $J^P = 0^-, 1^-, 2^-$ , especially those neutral ones with either  $C = +$  or  $C = -$ . Those states with  $J^{PC} = 0^{--}, 1^{-+}$  are exotic. They may exist with very reasonable coupling constants. For example, the  $J^{PC} = 0^{--}$  state is shown in Fig. 2.

The non-strange P-wave  $(0^+, 1^+)$  heavy mesons are very broad with a width around several hundred MeV [22]. Instead of forming a stable molecular state, the system containing one non-strange P-wave heavy meson may decay rapidly. Experimental identification of such a molecular state may be difficult. The attractive interaction between the meson pair may lead to a possible threshold enhancement in the production cross section.

In contrast, the P-wave charm-strange mesons  $D_{s0}(2317)$  and  $D_{s1}(2460)$  lie below the  $DK$  and  $D^*K$  threshold respectively. They are extremely narrow because their strong decays violate the isospin symmetry. The future experimental observation of the possible heavy molecular states composed of  $D_s/D_s^*$  and  $D_{s0}(2317)/D_{s1}(2460)$  may be feasible if they really exist.

There may exist (1) two  $0^-$  states around 4.25 GeV with different C-parity; (2) two  $0^-$  states around 4.5 GeV with different C-parity; (3) two  $2^-$  states around 4.5 GeV with different C-parity; (4) four  $1^-$  states around 4.35 GeV with different C-parity; (5) two  $1^-$  states around 4.5 GeV with different C-parity. The three neutral  $J^{PC} = 1^{--}$  states may be searched for via the initial state radiation technique. We notice that they are rather close to those  $1^{--}$  states observed by Belle around this mass region. The other states might be produced from  $B$  or  $B_s$  decays if kinematically allowed or at other possible facilities such as RHIC, Tevatron and LHCb.

The dominant decay modes of the above states are the open-charm modes  $D_s^{(*)}\bar{D}_s^{(*)}$  if angular momentum conservation, parity and C-parity symmetry allow. The other characteristic decay modes are the hidden-charm modes containing one  $J/\psi$ , or  $\eta_c$  or  $\chi_{cJ}$  etc. One may easily exhaust the possible final states according to C/P parity and angular momentum conservation and kinematical considerations. For those non-exotic states, they may be significantly narrower than the conventional charmonium around the same mass region because of their molecular nature. The manifestly exotic states may be searched for through their quantum number.

### Acknowledgment

The authors thank Wei-Zhen Deng for useful discussions. This project is supported by the National Natural Science Foundation of China under Grants No. 10625521, No. 10721063, No. 10705001, the Ministry of Science and Technology of China (2009CB825200) and the Ministry of Education of China (FANEDD under Grants No. 200924, DPFHIE under Grants No. 20090211120029, NCET under Grants No. NCET-10-0442).

- 
- [1] S. K. Choi et al., Phys. Rev. Lett. **91**, 262001 (2003).
  - [2] S. K. Choi et al., Phys. Rev. Lett. **94**, 182002 (2005).
  - [3] B. Aubert et al., BABAR Collaboration, Phys. Rev. Lett. **95**, 142001 (2005).
  - [4] C. Z. Yuan et al., Belle Collaboration, Phys. Rev. Lett. **99**, 182004 (2007).
  - [5] S. Uehara et al., Phys. Rev. Lett. **96**, 082003 (2006).
  - [6] K. Abe et al., Phys. Rev. Lett. **98**, 082001 (2007).
  - [7] B. Aubert et al., BABAR Collaboration, Phys. Rev. Lett. **98**, 212001 (2007).
  - [8] X. L. Wang et al., Belle Collaboration, Phys. Rev. Lett. **99**, 142002 (2007).
  - [9] S. K. Choi et al., Belle Collaboration, Phys. Rev. Lett. **100**, 142001 (2008).
  - [10] R. Mizuk et al., Belle Collaboration, Phys. Rev. D **78**, 072004 (2008).
  - [11] T. Aaltonen et al., CDF Collaboration, Phys. Rev. Lett. **102**, 242002 (2009).
  - [12] E. S. Swanson, Phys. Lett. B **598**, 197 (2004); E. S. Swanson, Phys. Lett. B **588**, 189 (2004); T. Fernandez-Carames, A. Valcarce, and J. Vijande, Phys. Rev. Lett. **103**, 222001 (2009).
  - [13] F. E. Close and C. Downum, Phys. Rev. Lett. **102**, 242003 (2009); F. E. Close, C. Downum, and C. E. Thomas, arXiv:1001.2553v1 [hep-ph].
  - [14] S. H. Lee, A. Mihara, F. Navarra, and M. Nielsen, Phys. Lett. B **661**, 28 (2008); C. Meng and K. T. Chao, arXiv:0708.4222 [hep-ph]; G. J. Ding, arXiv:0711.1485 [hep-ph].
  - [15] N. Mahajan Phys. Lett. B **679**, 228 (2009); T. Branz, T. Gutsche, and V. E. Lyubovitskij, Phys. Rev. D **80**, 054019 (2009); G. J. Ding, Eur. Phys. J. C **64** 297 (2009).
  - [16] X. Liu, Z. G. Luo, Y. R. Liu, Shi-Lin Zhu, Eur. Phys. J. C **61**, 411 (2009), arXiv:0808.0073 [hep-ph].
  - [17] Y. R. Liu, X. Liu, W. Z. Deng, Shi-Lin Zhu, Eur. Phys. J. C **56**, 63 (2008), arXiv:0801.3540 [hep-ph].
  - [18] X. Liu, Y.R. Liu, W. Z. Deng, and S. L. Zhu, Phys. Rev. D **77**, 094015 (2008).
  - [19] X. Liu, Y.R. Liu, W. Z. Deng, and S. L. Zhu, Phys. Rev. D **77**, 034003 (2008).
  - [20] X. Liu and S. L. Zhu, Phys. Rev. D **80**, 017502 (2009).
  - [21] B. Hu, X.L. Chen, Z.G. Luo, P.Z. Huang, S.L. Zhu, P.F. Yu and X. Liu, arXiv:1004.4032 [hep-ph].
  - [22] C. Amsler et al., (Particle Data Group), Phys. Lett. B **667**, 1 (2008).
  - [23] R. Casalbuoni, A. Deandrea, N. Di Bartolomeo, R. Gatto, F. Feruglio and G. Nardulli, Phys. Rept. **281**, 145 (1997) [arXiv:hep-ph/9605342].
  - [24] P. Z. Huang, L. Zhang, Shi-Lin Zhu, Phys. Rev. D **80**, 014023 (2009).

## Appendix

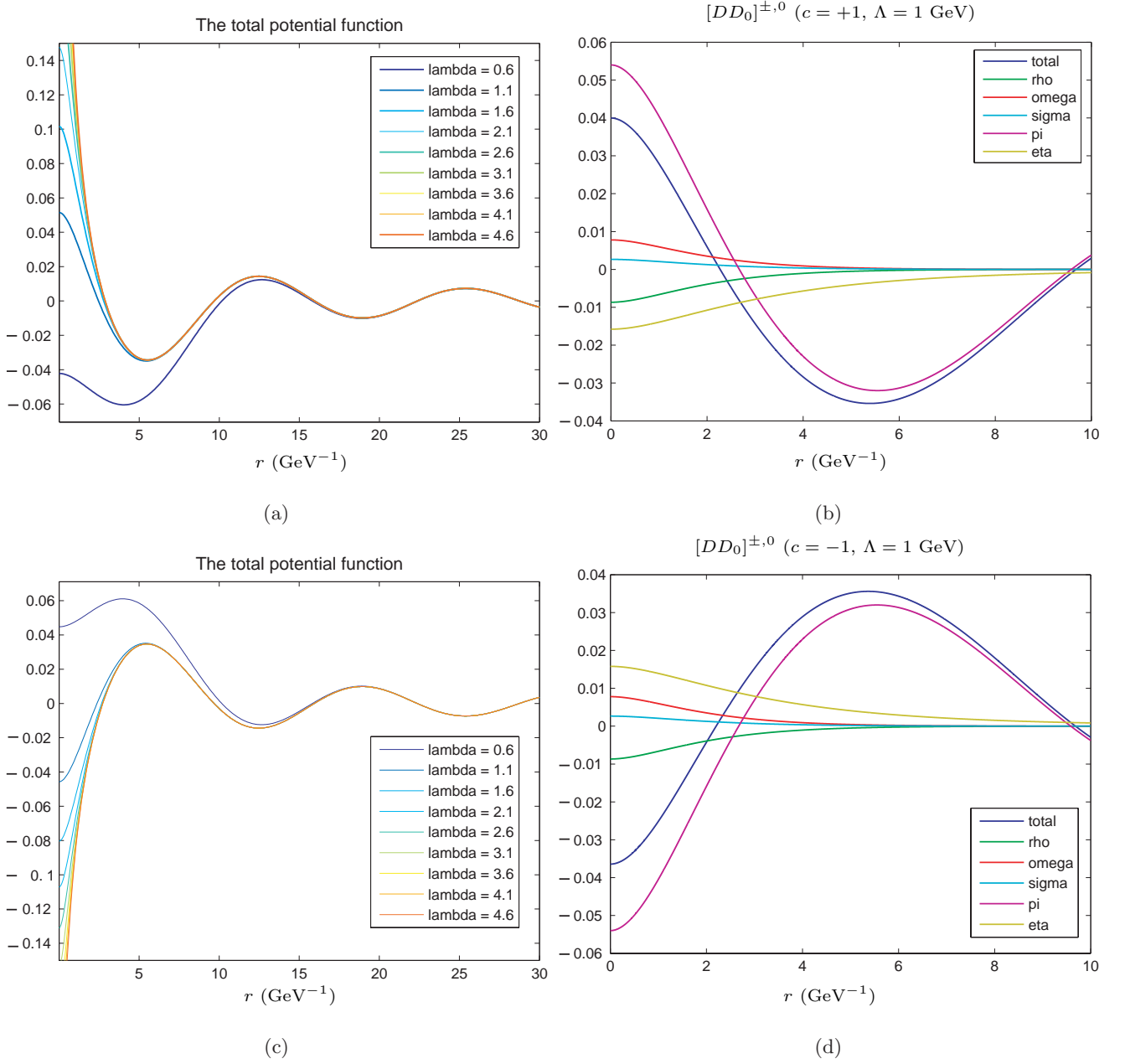
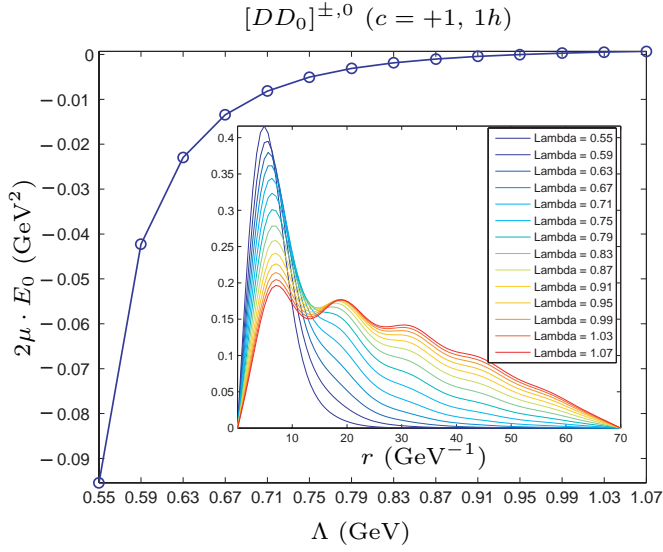
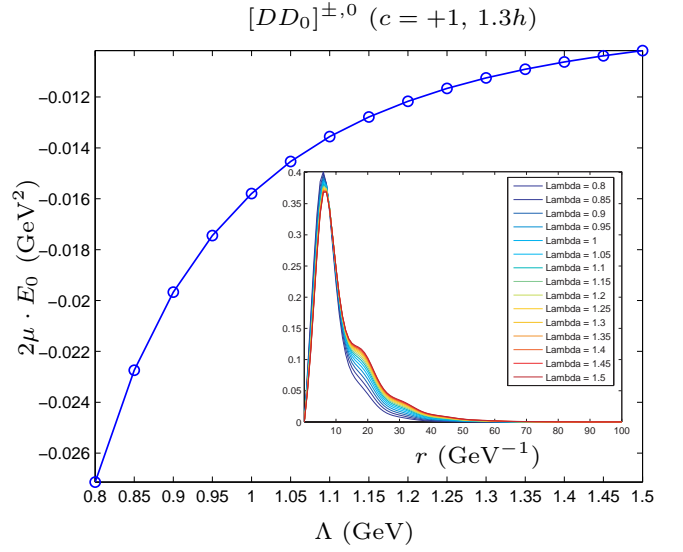


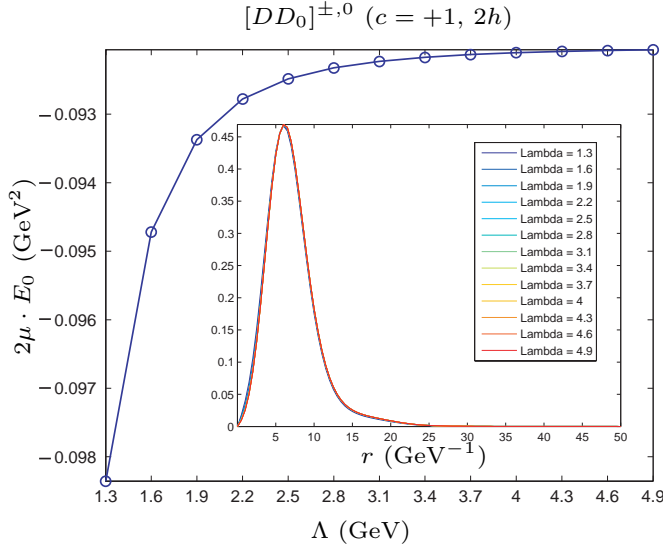
FIG. 1: (a) The variation of the total potential of the  $[DD_0]^{\pm,0}$  system ( $c = +1$ ) with  $r$  and  $\Lambda$ ; (b) the exchange potentials of the  $\pi$ ,  $\eta$ ,  $\sigma$ ,  $\rho$ ,  $\omega$  mesons of the  $[DD_0]^{\pm,0}$  system ( $c = +1$ ) with  $\Lambda = 1 \text{ GeV}$ ; (c) the variation of the total potential of the  $[DD_0]^{\pm,0}$  system ( $c = -1$ ) with  $r$  and  $\Lambda$ ; (d) the exchange potentials of the  $\pi$ ,  $\eta$ ,  $\sigma$ ,  $\rho$ ,  $\omega$  mesons of the  $[DD_0]^{\pm,0}$  system ( $c = -1$ ) with  $\Lambda = 1 \text{ GeV}$ . The above potentials are obtained when  $g_\sigma g'_\sigma > 0$  and  $\beta\beta' > 0$ . Here,  $|h| = 0.56$ ,  $|g_\sigma| = 0.76$ ,  $|g'_\sigma| = 0.76$ ,  $|\beta| = 0.909$  and  $|\beta'| = 0.533$ .



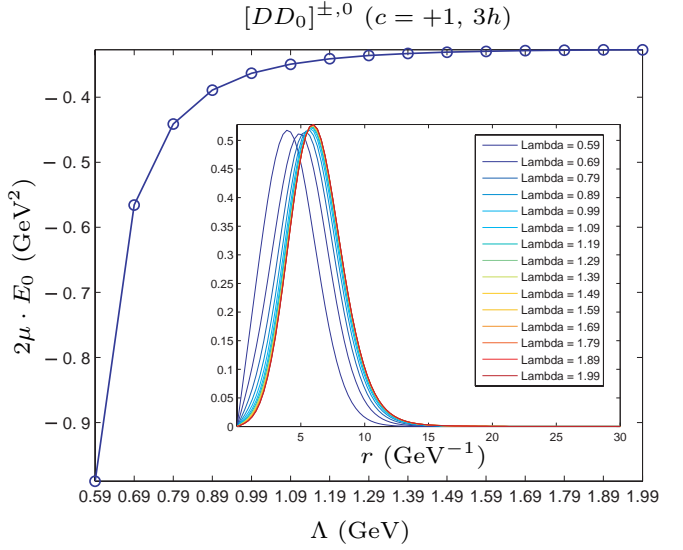
(a)



(b)



(c)



(d)

FIG. 2: The dependence of the binding energy of the  $[DD_0]^{\pm,0}$  system ( $c = +1$ ) on  $\Lambda$  and the wave function of this system. Here, we only consider the single  $\pi$  exchange potential. (a), (b), (c) and (d) correspond to the case of  $1h$ ,  $1.3h$ ,  $2h$  and  $3h$  with  $|h| = 0.56$  respectively.

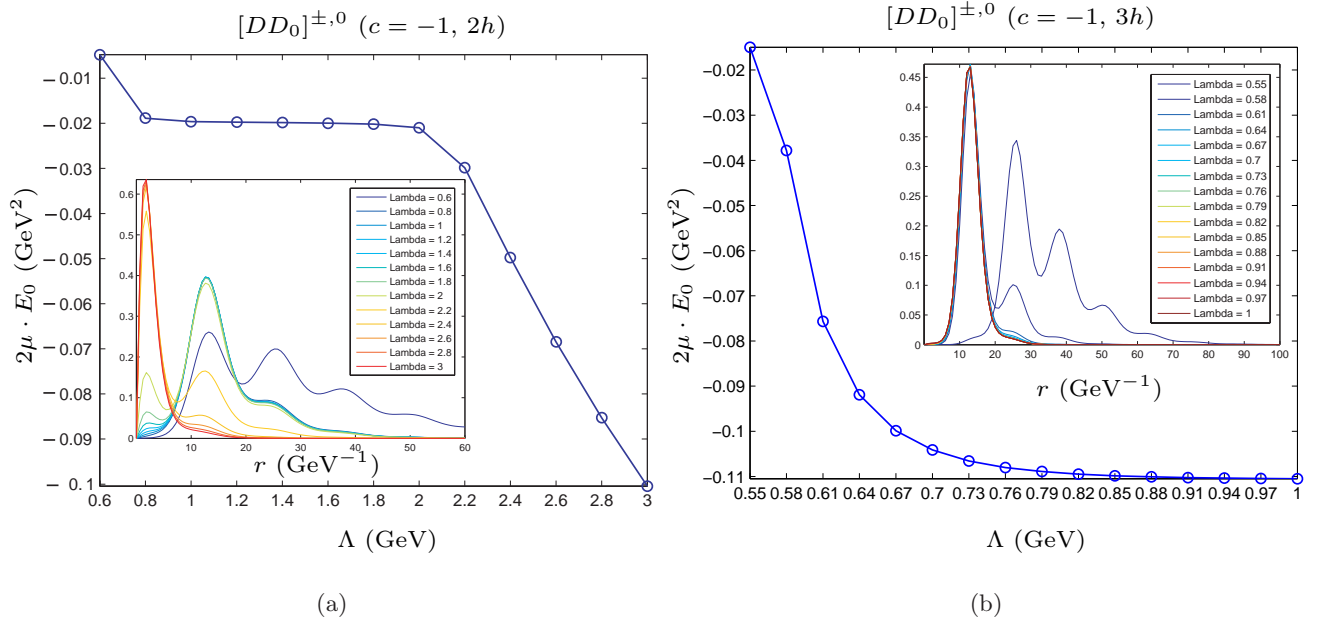


FIG. 3: The dependence of the binding energy of  $[DD_0]^{\pm,0}$  system ( $c = -1$ ) on  $\Lambda$  and the wave function of this system. Here, we only consider the single  $\pi$  exchange potential. (a) and (b) correspond to the case of  $2h$  and  $3h$  with  $|h| = 0.56$  respectively. When taking  $1h$ , we can not find the bound state solution.

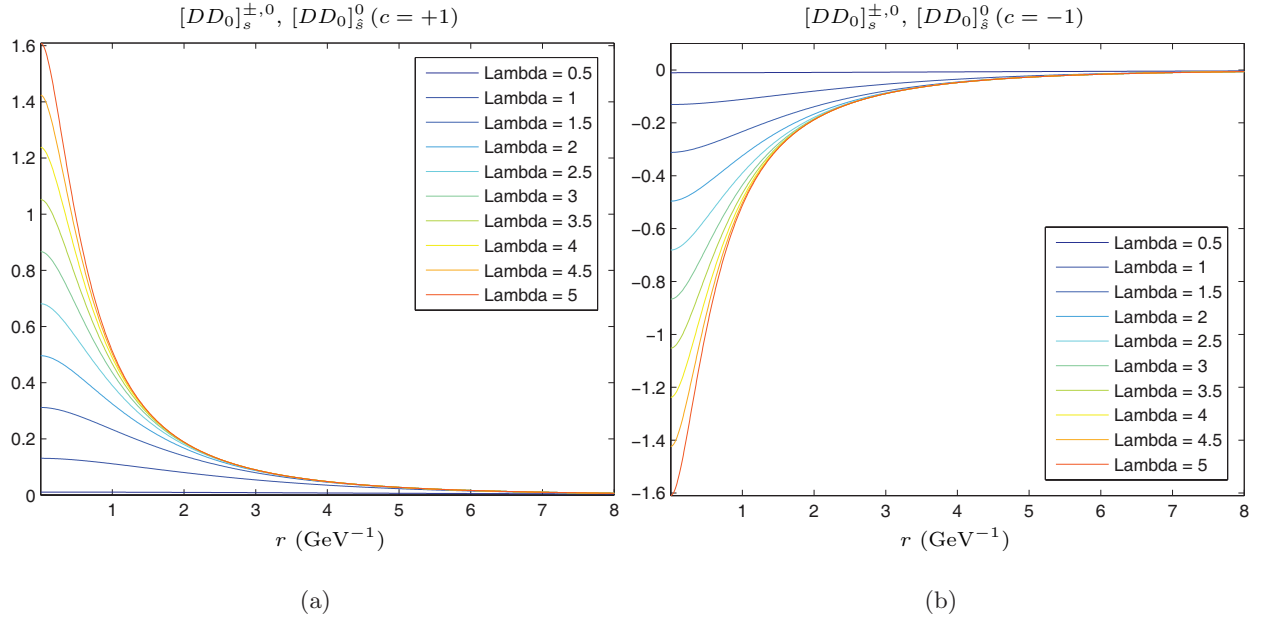


FIG. 4: (a) The variation of the total potential of the  $[DD_0]_s^{\pm,0}, [DD_0]_s^0$  system ( $c = +1$ ) with  $r$  and  $\Lambda$ ; (b) The variation of the total potential of the  $[DD_0]_s^{\pm,0}, [DD_0]_s^0$  system ( $c = -1$ ) with  $r$  and  $\Lambda$ . Here, we take  $|h| = 0.56$ .

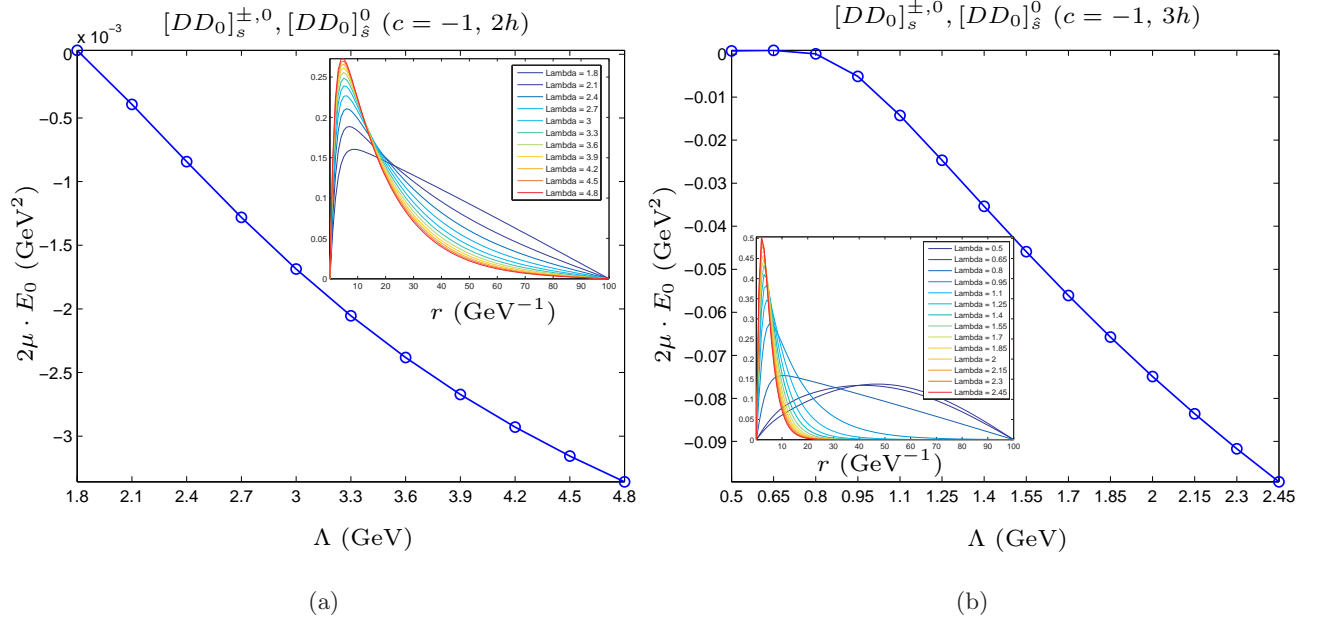


FIG. 5: The dependence of the binding energy of the  $[DD_0]_s^{\pm,0}, [DD_0]_s^0$  system ( $c = -1$ ) on  $\Lambda$  and the wave function of this system. Here, we only consider the single  $\eta$  exchange potential. (a) and (b) correspond to the case of  $2h$  and  $3h$  with  $|h| = 0.56$  respectively. When taking  $1h$ , we can not find the bound state solution.

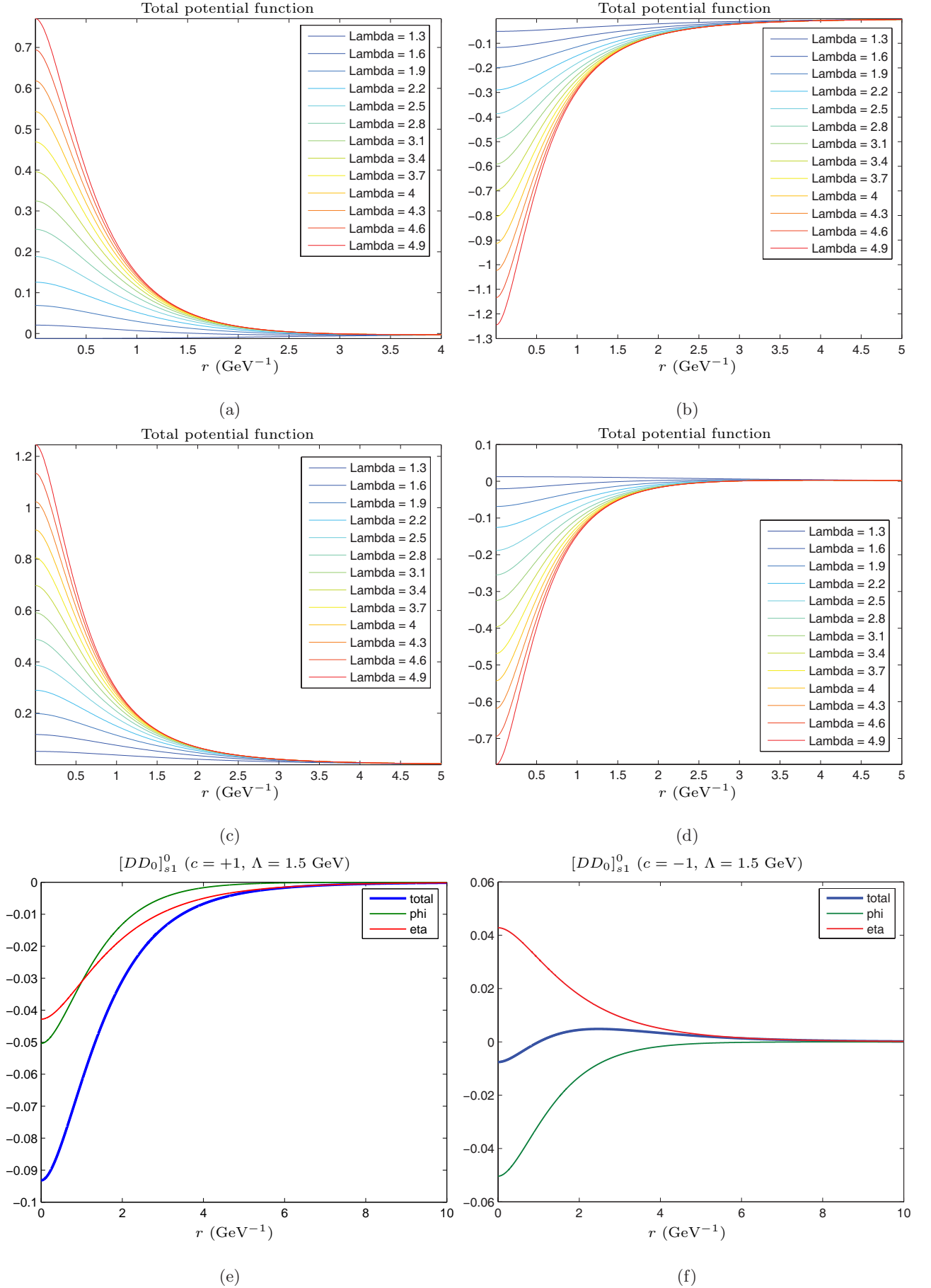
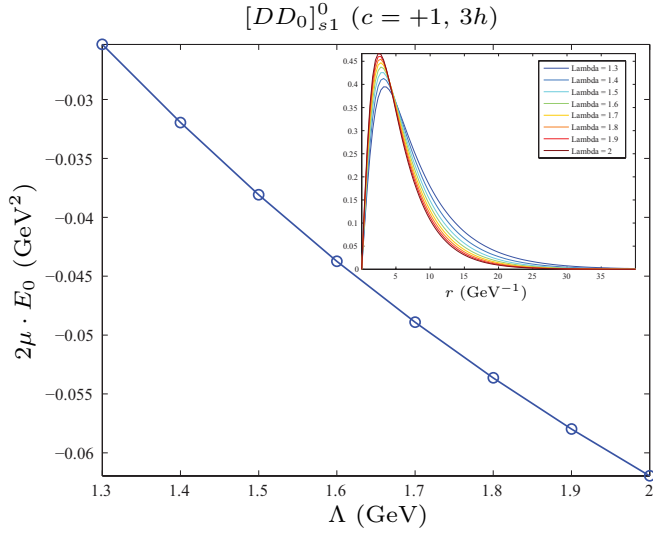
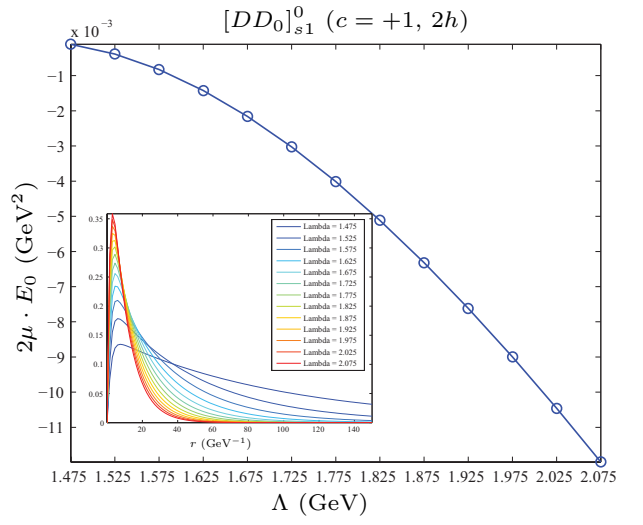


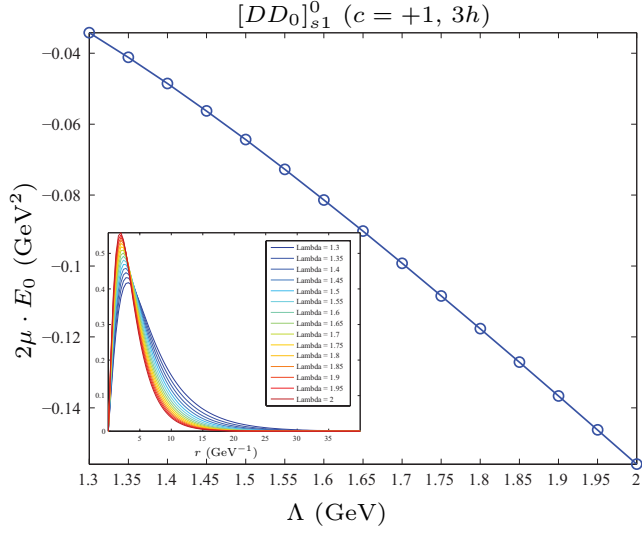
FIG. 6: (a), (b), (c) and (d) are the total potentials of the  $[DD_0]_{s1}^0$  systems with  $(c = +1, \beta\beta' > 0)$ ,  $(c = +1, \beta\beta' < 0)$ ,  $(c = -1, \beta\beta' > 0)$  and  $(c = -1, \beta\beta' < 0)$  respectively. Under taking  $\Lambda = 1.5 \text{ GeV}$ , (e) and (f) are the partial potentials of the  $[DD_0]_{s1}^0$  system with  $(c = +1, \beta\beta' < 0)$  and  $(c = -1, \beta\beta' < 0)$  respectively. Here, we take  $|h| = 0.56$ ,  $|\beta| = 0.909$  and  $|\beta'| = 0.533$ .



(a)



(b)



(c)

FIG. 7: The dependence of the binding energy of the  $[DD_0]_{s1}^0$  system ( $c = +1$ ) on  $\Lambda$  and the wave function of this system. Here, we consider the contribution of the  $\eta$  and  $\phi$  exchange potentials. (a) is for ( $c = +1, \beta\beta' > 0$ ); (b) and (c) are for ( $c = +1, \beta\beta' < 0$ ). When taking ( $c = -1, \beta\beta' < 0$ ), we can not find the bound state solution. Here, we take  $|h| = 0.56$ ,  $|\beta| = 0.909$  and  $|\beta'| = 0.533$ .

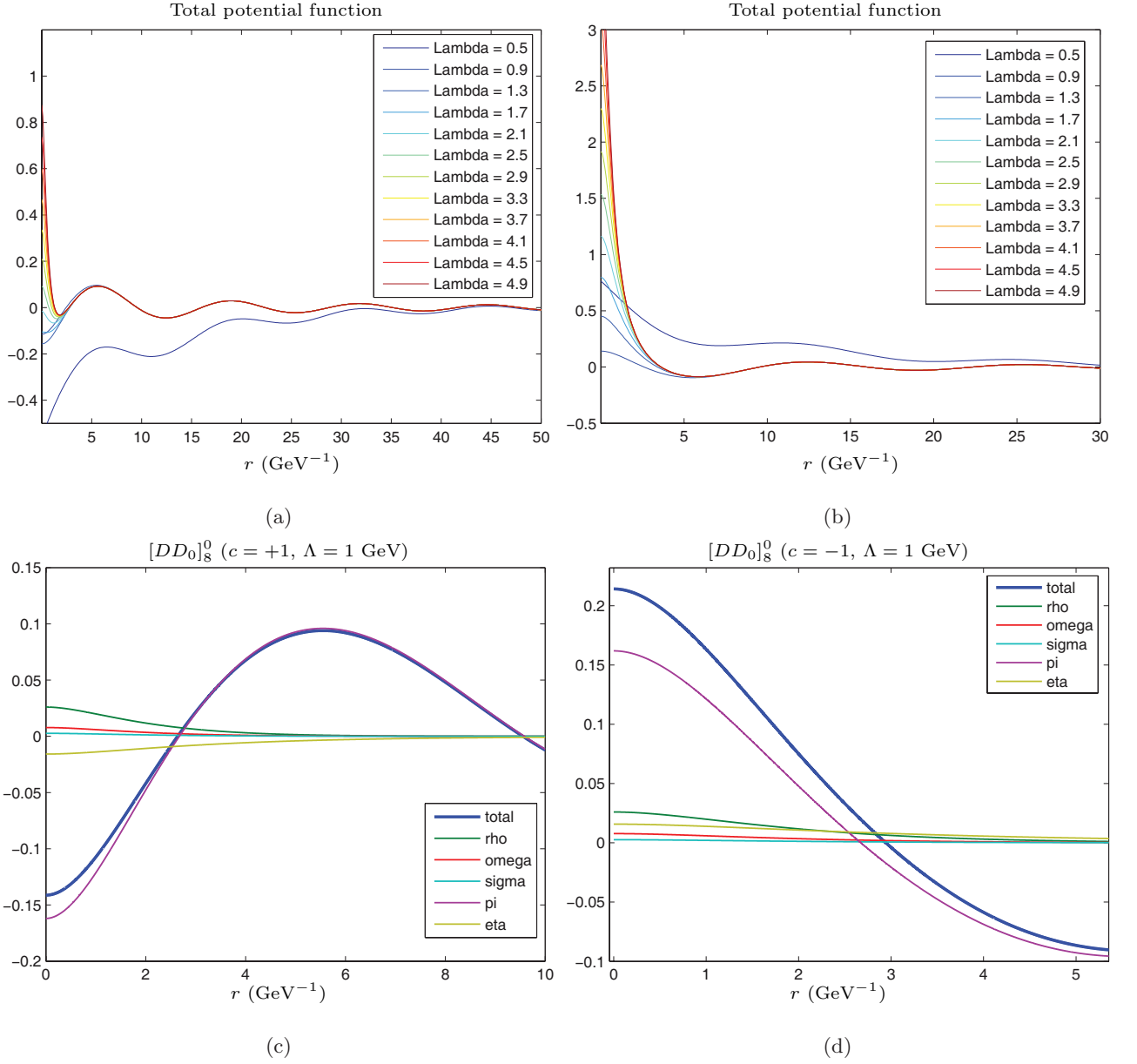


FIG. 8: (a) and (b) are the total potentials of the  $[DD_0]_8^0$  systems with  $c = +1$  and  $c = -1$  respectively. With  $\Lambda = 1$  GeV, diagrams (c) and (d) illustrate the partial potentials of the  $[DD_0]_8^0$  system with  $c = +1$  and  $c = -1$  respectively. The above potentials are obtained with  $g_\sigma g'_\sigma > 0$  and  $\beta\beta' > 0$ . Here,  $|h| = 0.56$ ,  $|g_\sigma| = 0.76$ ,  $|g'_\sigma| = 0.76$ ,  $|\beta| = 0.909$  and  $|\beta'| = 0.533$ .

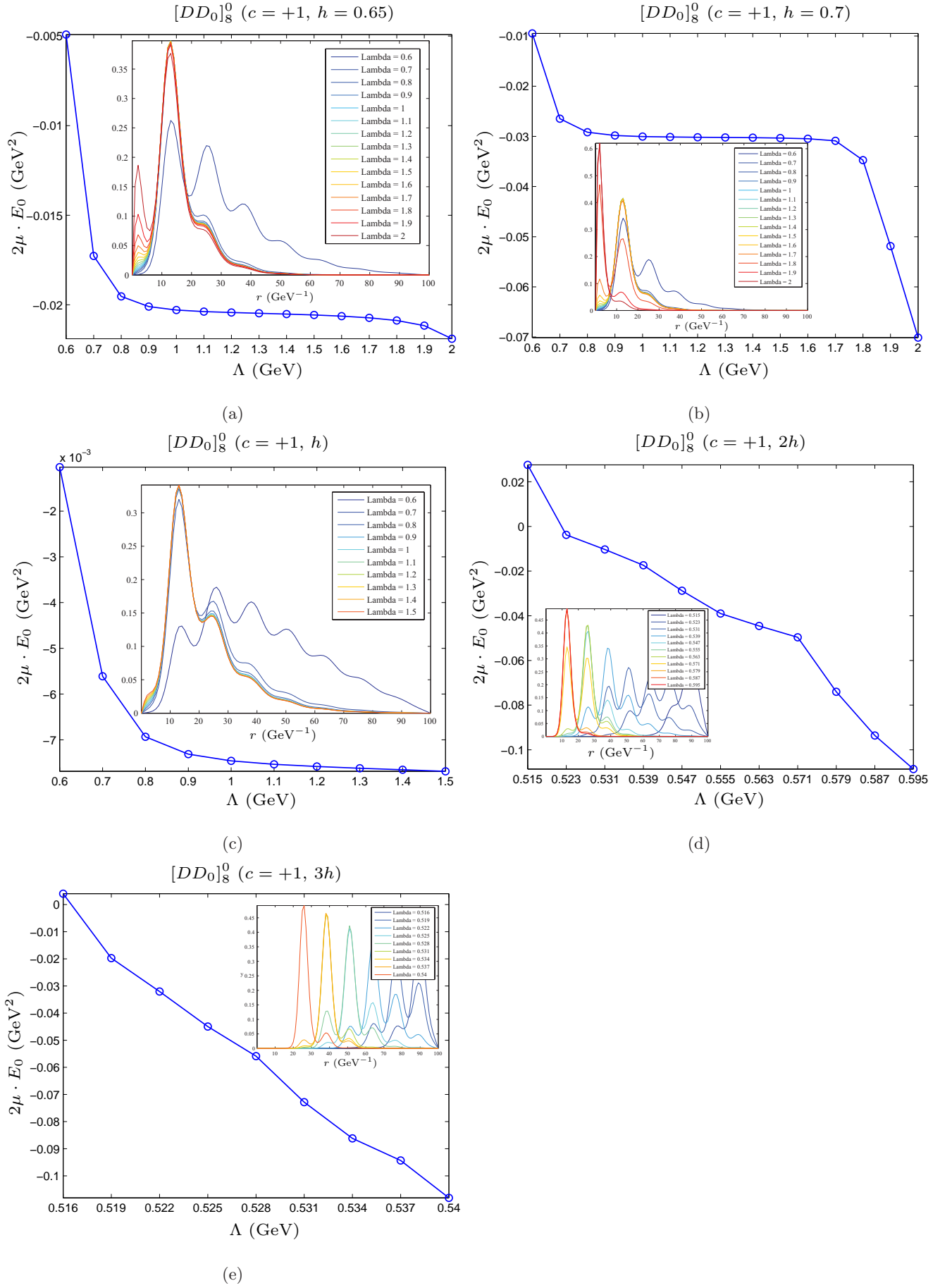


FIG. 9: The dependence of the binding energy of the  $[DD_0]_8^0$  system ( $c = +1$ ) on  $\Lambda$  and the wave function of this system. Here, we only consider the contribution of the  $\pi$  exchange potentials. We take different values of  $h$ , in diagrams (a)-(e). The absolute value of  $h$  in  $1h, 2h, 3h$  is 0.56.

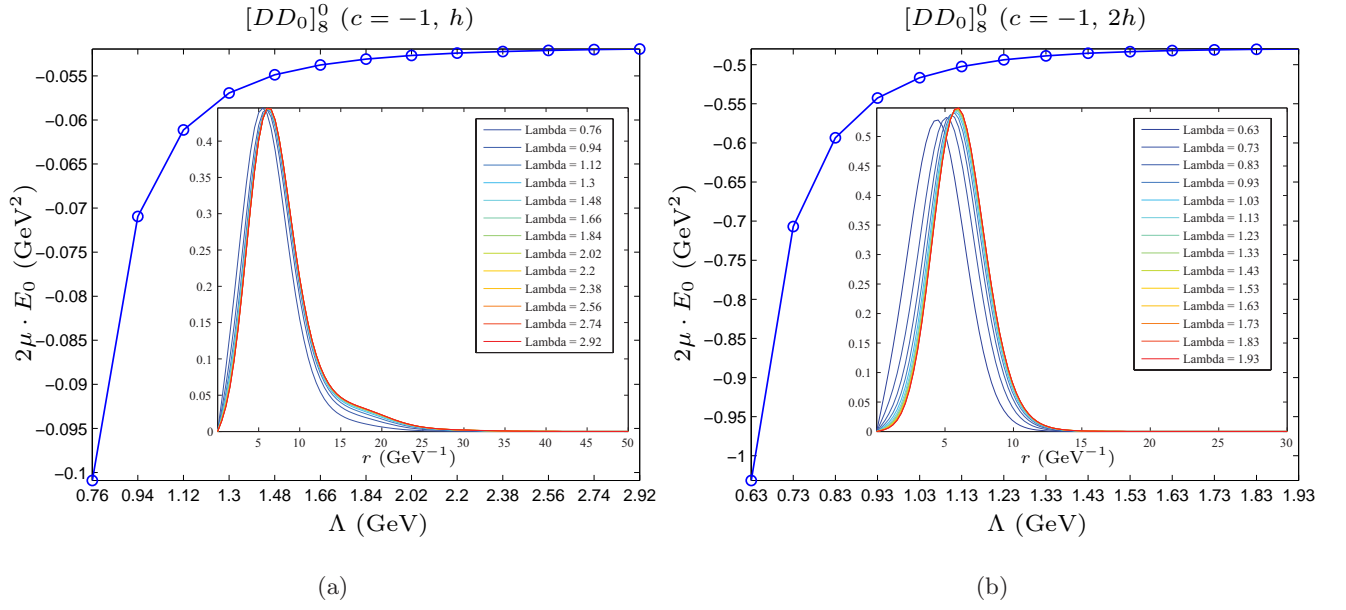


FIG. 10: The binding energy of the  $[DD_0]_8^0$  system ( $c = -1$ ) and the wave function of this system. Here, we only consider the  $\pi$  exchange potential with  $1h, 2h$  in diagrams (a)-(c) respectively. Here,  $|h| = 0.56$ .

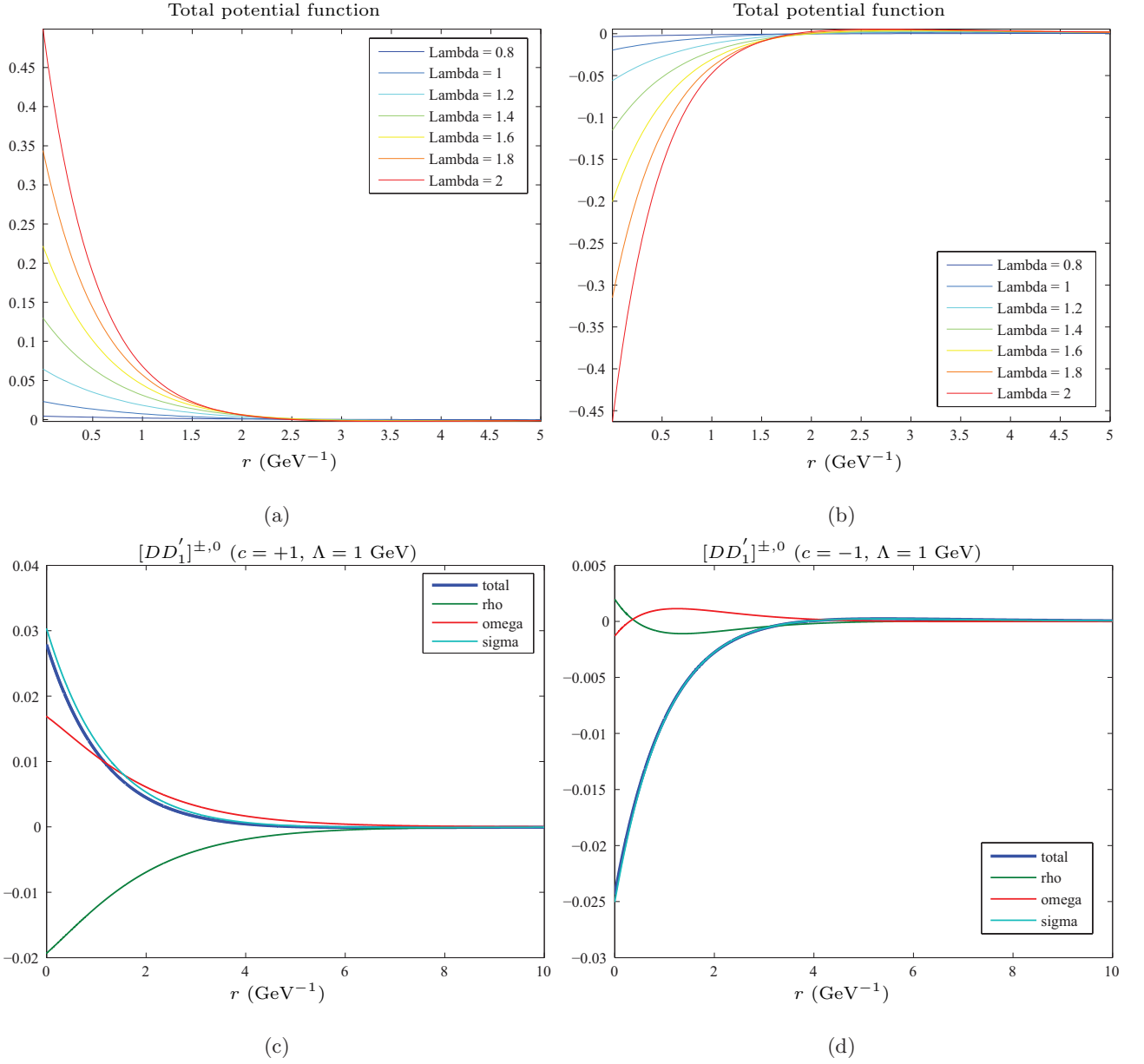


FIG. 11: (a) The variation of the total potential of the  $[DD'_1]^{\pm,0}$  system ( $c = +1$ ) with  $r$  and  $\Lambda$ ; (b) the variation of the total potential of the  $[DD'_1]^{\pm,0}$  system ( $c = -1$ ) with  $r$  and  $\Lambda$ ; (c) the exchange potentials of the  $\sigma$ ,  $\rho$ ,  $\omega$  mesons of the  $[DD'_1]^{\pm,0}$  system ( $c = +1$ ) with  $\Lambda = 1$  GeV; (d) the exchange potentials of the  $\sigma$ ,  $\rho$ ,  $\omega$  mesons of the  $[DD'_1]^{\pm,0}$  system ( $c = -1$ ) with  $\Lambda = 1$  GeV. The above potentials are obtained with  $g_\sigma g'_\sigma > 0$ ,  $\beta\beta' > 0$  and  $\zeta\varpi > 0$ . Here,  $|g_\sigma| = 0.76$ ,  $|g'_\sigma| = 0.76$ ,  $|h_\sigma| = 0.323$ ,  $|\beta| = 0.909$  and  $|\beta'| = 0.533$ ,  $\zeta = 0.727$  and  $\varpi = 0.364$ .

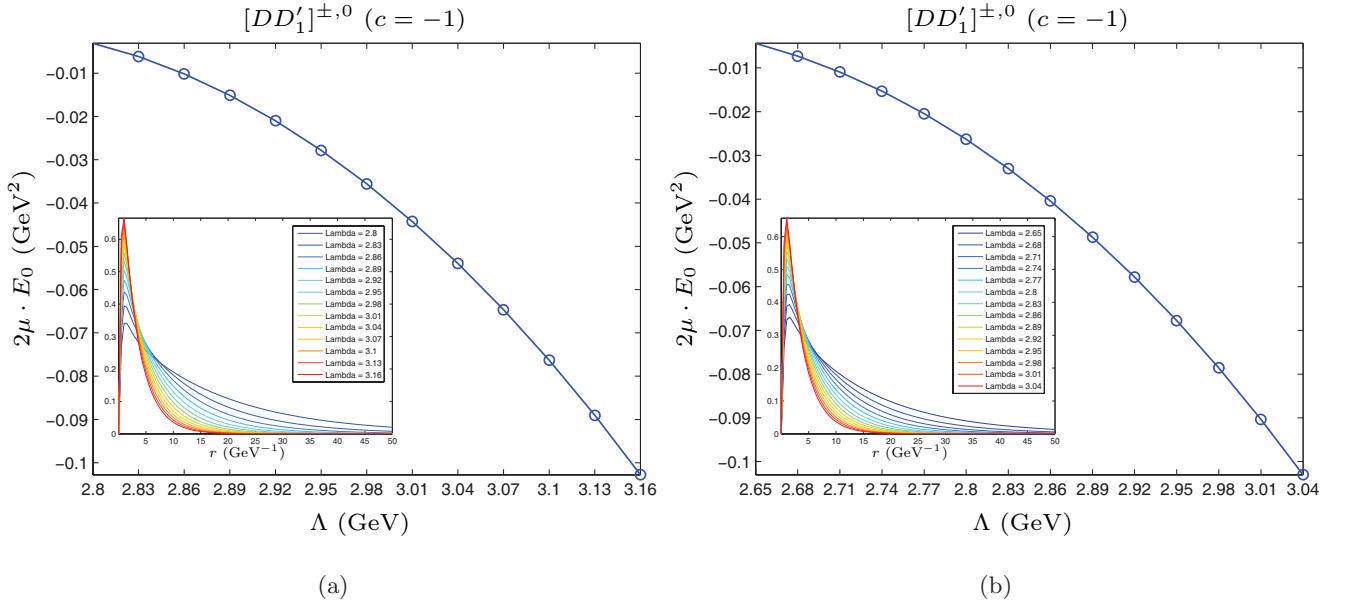


FIG. 12: The binding energy of the  $[DD'_1]^{\pm,0}$  system ( $c = -1$ ) and the wave function of this system with  $2h_\sigma$ . Here, we only consider the  $\sigma$  exchange potential. (a) and (b) correspond to the case of  $g_\sigma g'_\sigma > 0$  and  $g_\sigma g'_\sigma < 0$  with  $|h_\sigma| = 0.323$ ,  $|g_\sigma| = 0.76$  and  $|g'_\sigma| = 0.76$  respectively.

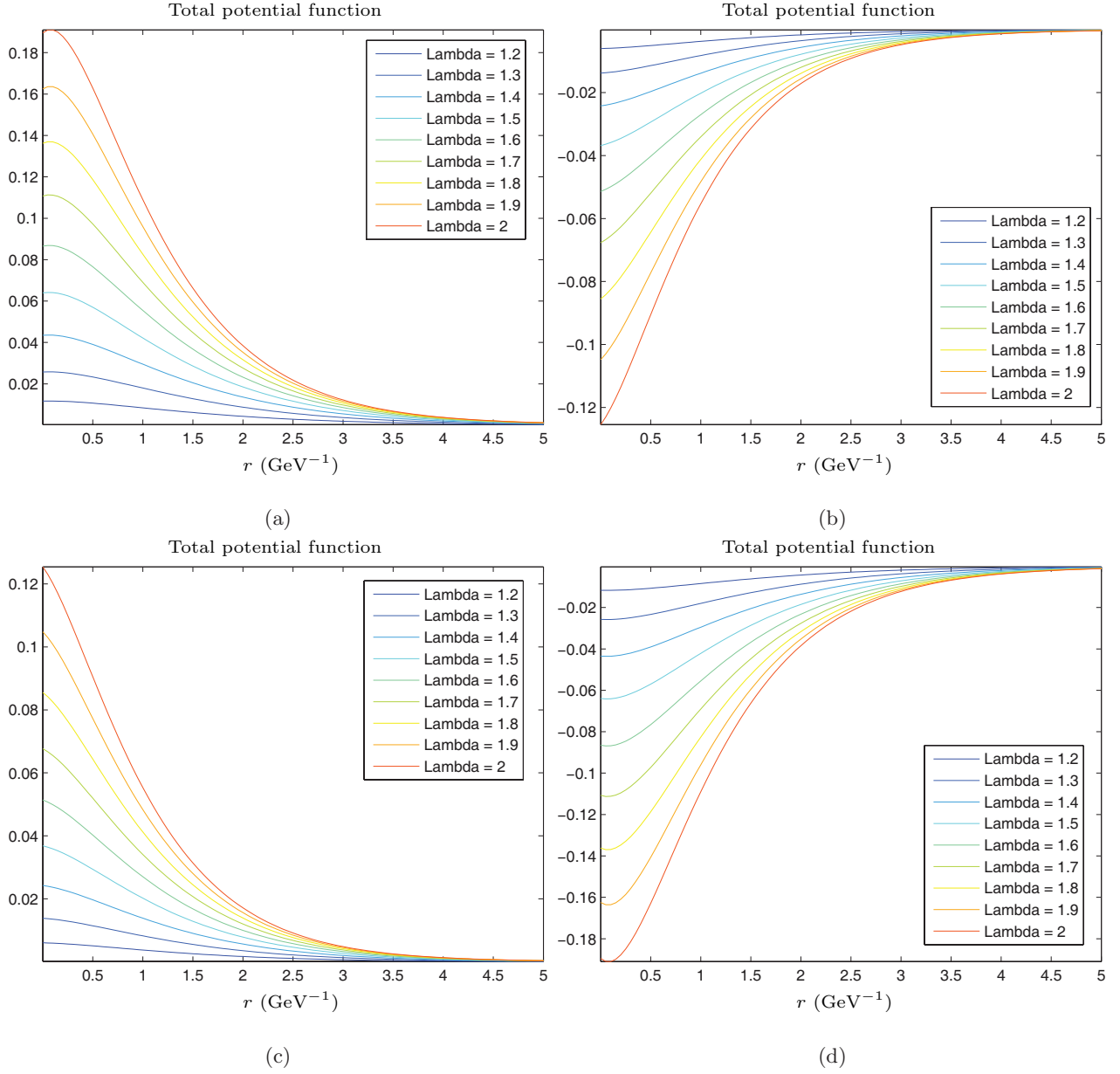


FIG. 13: (a), (b), (c) and (d) are the potentials of the  $[PP]_{s1}^0$  with  $(c = +1, \beta\beta' > 0)$ ,  $(c = +1, \beta\beta' < 0)$ ,  $(c = -1, \beta\beta' > 0)$  and  $(c = -1, \beta\beta' < 0)$ , respectively. Here, we take  $\zeta\varpi > 0$  with  $|\beta| = 0.909$ ,  $|\beta'| = 0.533$ ,  $|\zeta| = 0.727$  and  $|\varpi| = 0.364$ .

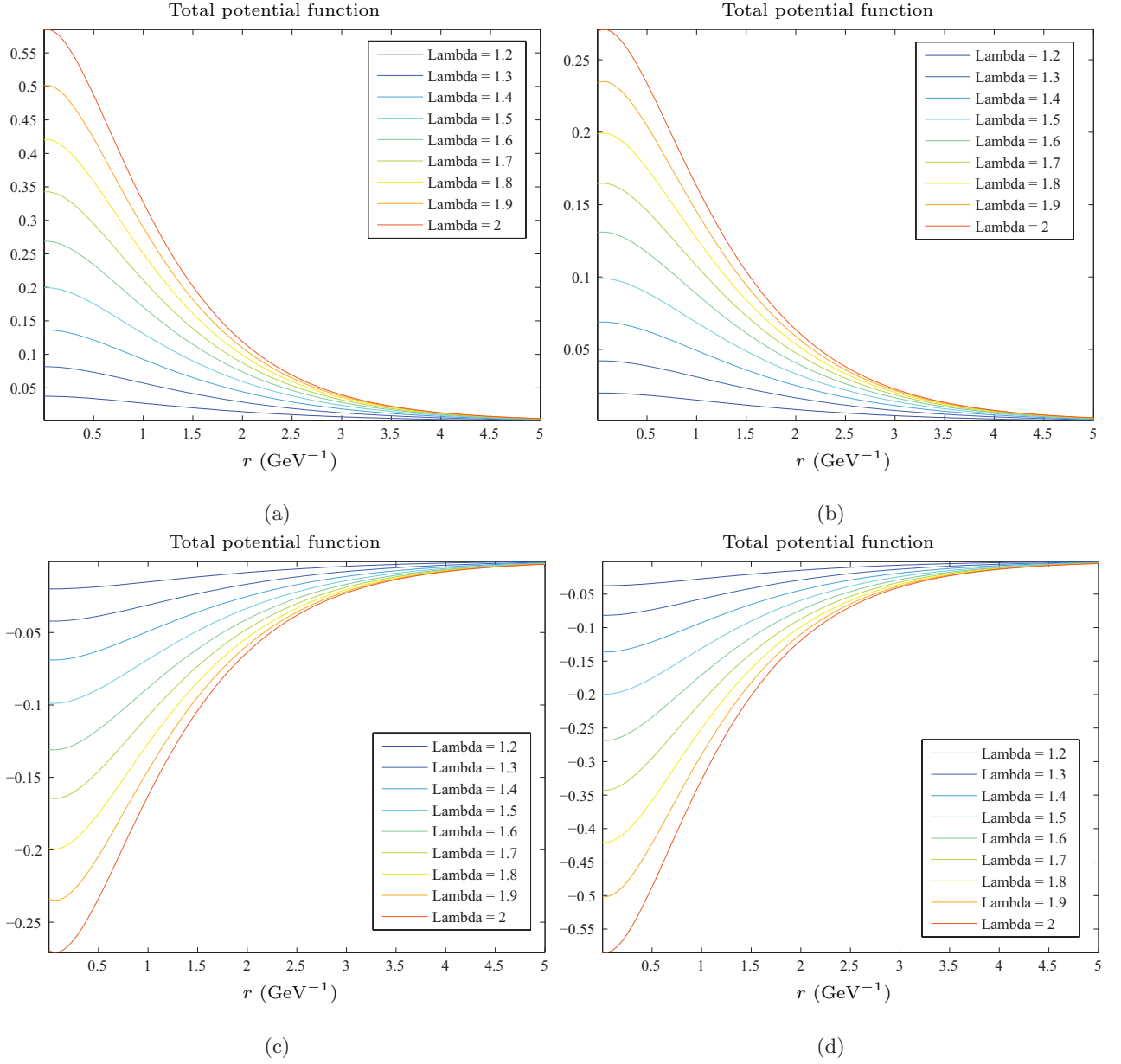


FIG. 14: (a), (b), (c) and (d) are the potentials of the  $[PP_1]_{s1}^0$  with  $(c = +1, \beta\beta' > 0)$ ,  $(c = +1, \beta\beta' < 0)$ ,  $(c = -1, \beta\beta' > 0)$  and  $(c = -1, \beta\beta' < 0)$ , respectively. Here, we take  $\zeta\varpi < 0$  with  $|\beta| = 0.909$ ,  $|\beta'| = 0.533$ ,  $|\zeta| = 0.727$  and  $|\varpi| = 0.364$ .

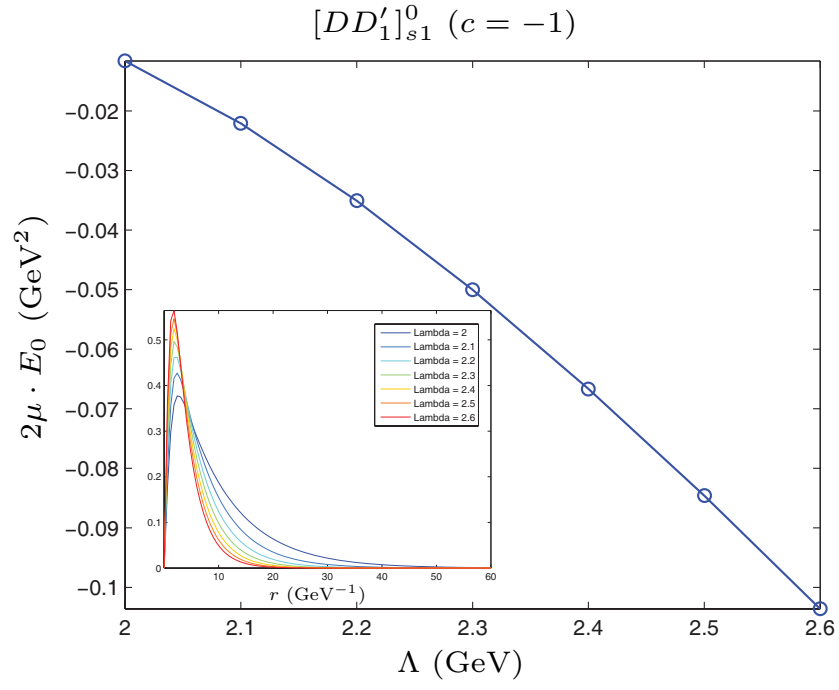


FIG. 15: The dependence of the binding energy of the  $[PP'_1]_{s1}^0$  system on  $\Lambda$  with  $c = -1$ ,  $\beta\beta' < 0$  and  $\zeta\varpi < 0$  with  $|\beta| = 0.909$ ,  $|\beta'| = 0.533$ ,  $|\zeta| = 0.727$  and  $|\varpi| = 0.364$ .

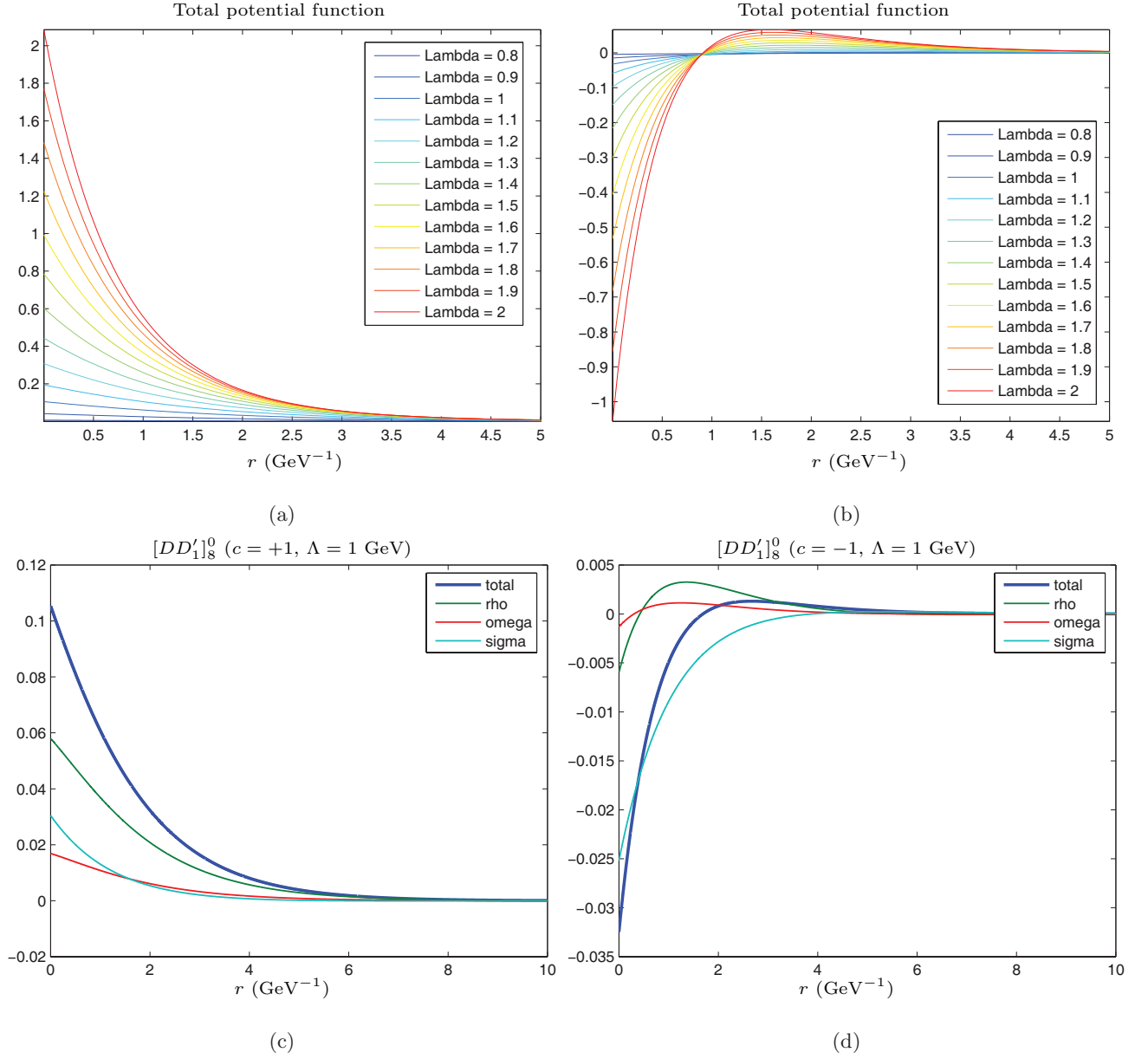


FIG. 16: (a) and (b) are the total potentials of the  $[PP'_1]_8^0$  system with  $c = +1$  and  $c = -1$  respectively when  $g_\sigma g'_\sigma > 0$ ,  $\beta\beta' > 0$  and  $\zeta\mu > 0$  with  $|\beta| = 0.909$ ,  $|\beta'| = 0.533$ ,  $|\zeta| = 0.727$  and  $|\varpi| = 0.364$ . With  $\Lambda = 1$  GeV, we show the comparison of the total potential and the  $\sigma$ ,  $\rho$ ,  $\omega$  exchange potentials, where (c) and (d) illustrate the result of the  $[PP'_1]_8^0$  system with  $c = +1$  and  $c = -1$  respectively.

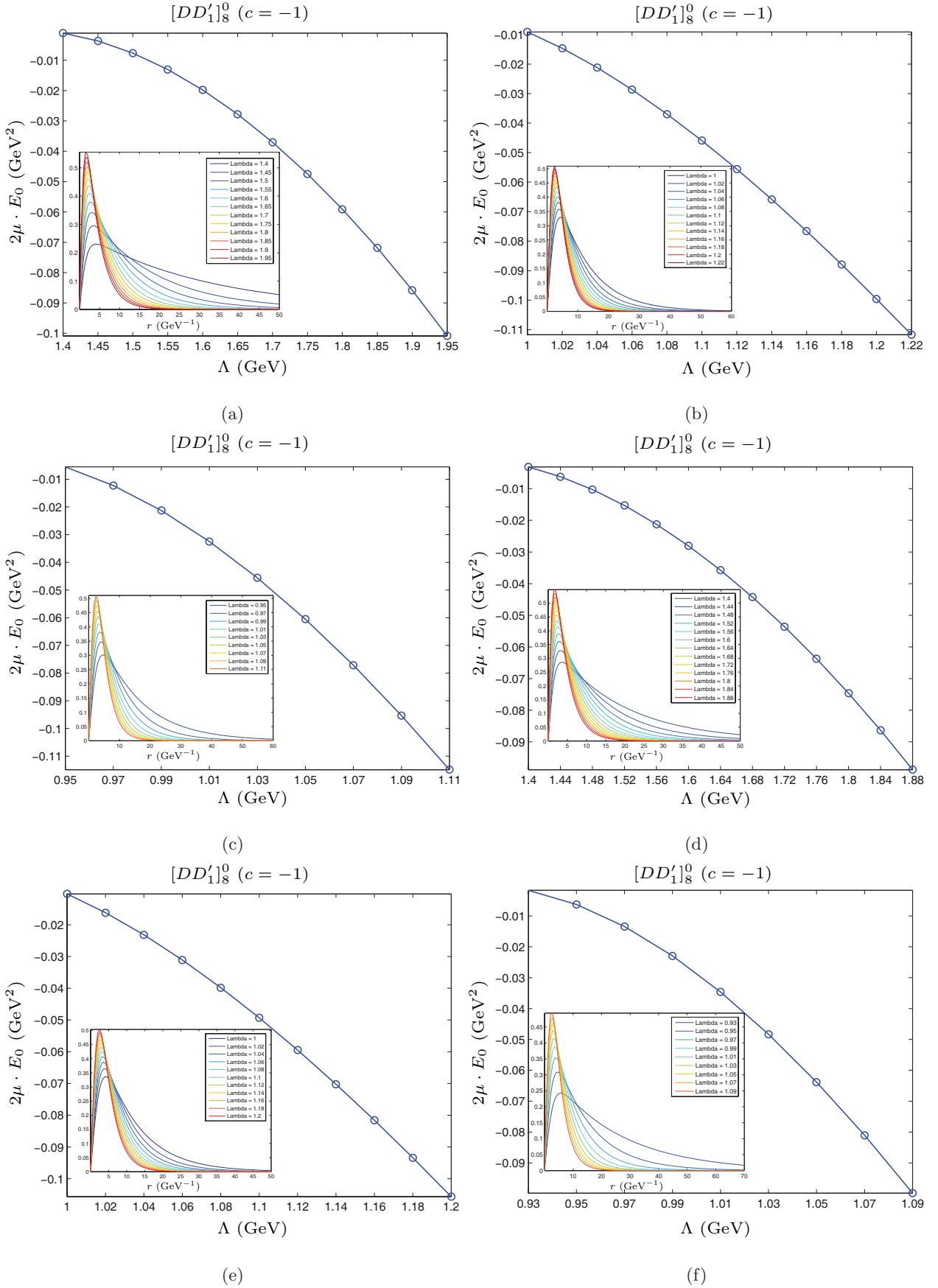


FIG. 17: The bound state solution of the  $[PP'_1]_8^0$  with  $c = -1$ . (a), (b), (c), (d), (e), and (f) correspond to the results with  $(g_\sigma g'_\sigma > 0, \beta\beta' < 0, \zeta\varpi > 0)$ ,  $(g_\sigma g'_\sigma > 0, \beta\beta' > 0, \zeta\varpi < 0)$ ,  $(g_\sigma g'_\sigma > 0, \beta\beta' < 0, \zeta\varpi < 0)$ ,  $(g_\sigma g'_\sigma < 0, \beta\beta' < 0, \zeta\varpi > 0)$ ,  $(g_\sigma g'_\sigma < 0, \beta\beta' > 0, \zeta\varpi < 0)$  and  $(g_\sigma g'_\sigma < 0, \beta\beta' < 0, \zeta\varpi < 0)$  respectively. When taking  $(g_\sigma g'_\sigma > 0, \beta\beta' > 0, \zeta\varpi > 0)$  or  $(g_\sigma g'_\sigma < 0, \beta\beta' > 0, \zeta\varpi > 0)$ , we can not find the bound state solution. Here,  $|g_\sigma| = 0.76$ ,  $|g'_\sigma| = 0.76$ ,  $|h_\sigma| = 0.323$ ,  $|\beta| = 0.909$  and  $|\beta'| = 0.533$ ,  $\zeta = 0.727$  and  $\varpi = 0.364$ .

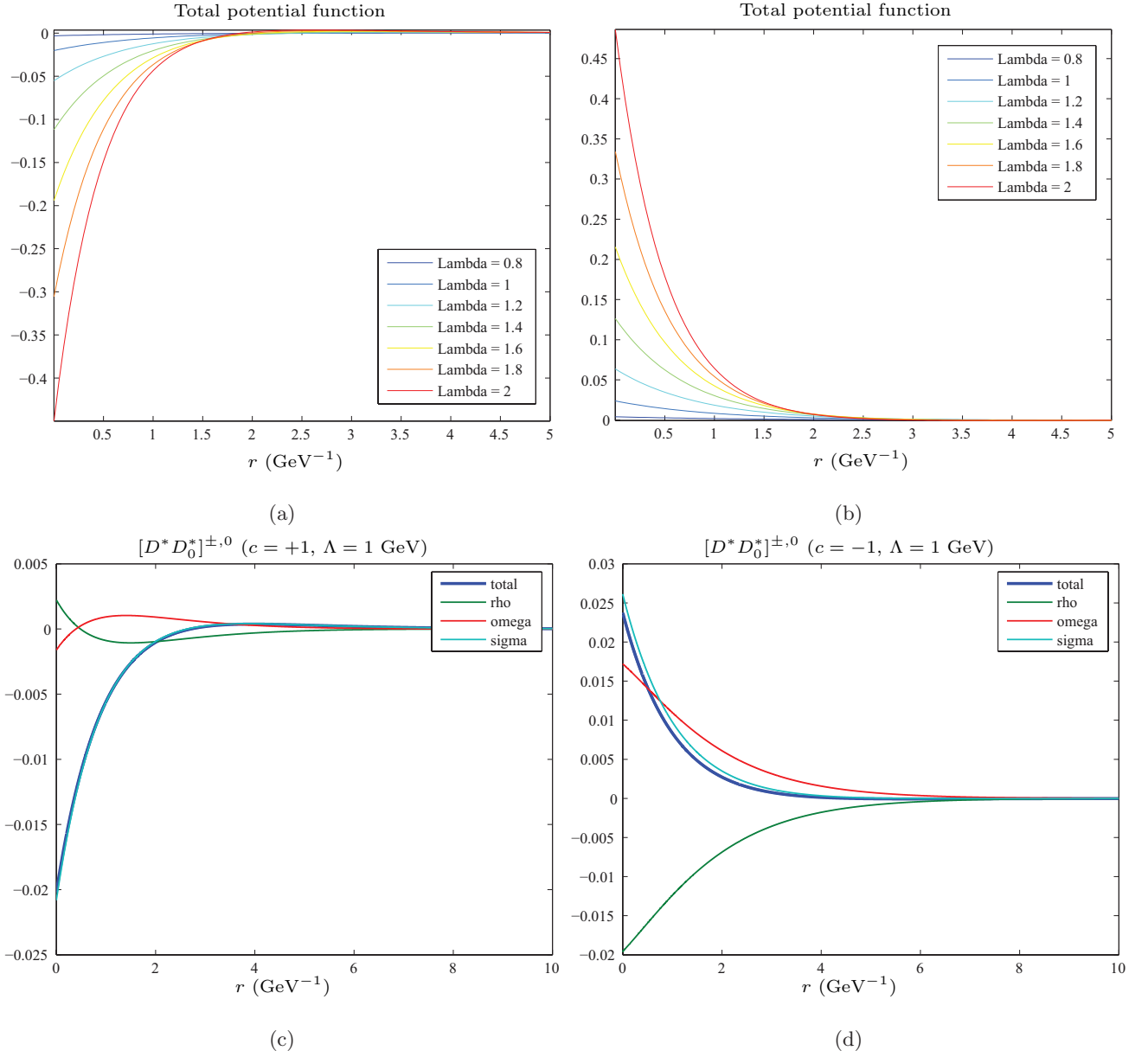


FIG. 18: (a) The variation of the total potential of the  $[D^* D_0^{*\pm,0}]$  system ( $c = +1$ ) with  $r$  and  $\Lambda$ ; (b) the variation of the total potential of the  $[D^* D_0^{*\pm,0}]$  system ( $c = -1$ ) with  $r$  and  $\Lambda$ ; (c) the exchange potentials of the  $\sigma$ ,  $\rho$ ,  $\omega$  mesons of the  $[DD_1^{\pm,0}]$  system ( $c = +1$ ) with  $\Lambda = 1$  GeV; (d) the exchange potentials of the  $\sigma$ ,  $\rho$ ,  $\omega$  mesons of the  $[D^* D_0^{*\pm,0}]$  system ( $c = -1$ ) with  $\Lambda = 1$  GeV. The above potentials are obtained with  $g_\sigma g'_\sigma > 0$ ,  $\beta\beta' > 0$  and  $\zeta\varpi > 0$ . Here,  $|g_\sigma| = 0.76$ ,  $|g'_\sigma| = 0.76$ ,  $|h_\sigma| = 0.32$ ,  $|\beta| = 0.909$  and  $|\beta'| = 0.533$ ,  $\zeta = 0.727$  and  $\varpi = 0.364$ .

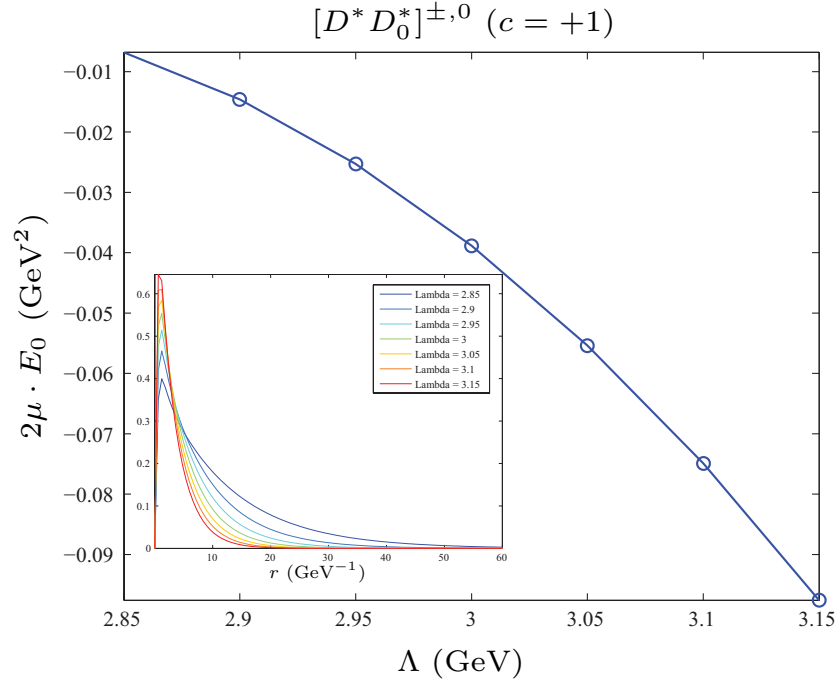


FIG. 19: The binding energy of the  $[D^* D_0^*]^{\pm,0}$  system ( $c = +1$ ) and its wave function with  $2h_\sigma$ . Here, we only consider the  $\sigma$  exchange potential and take  $g_\sigma g'_\sigma < 0$  with  $|h_\sigma| = 0.323$ ,  $|g_\sigma| = 0.76$  and  $|g'_\sigma| = 0.76$ .

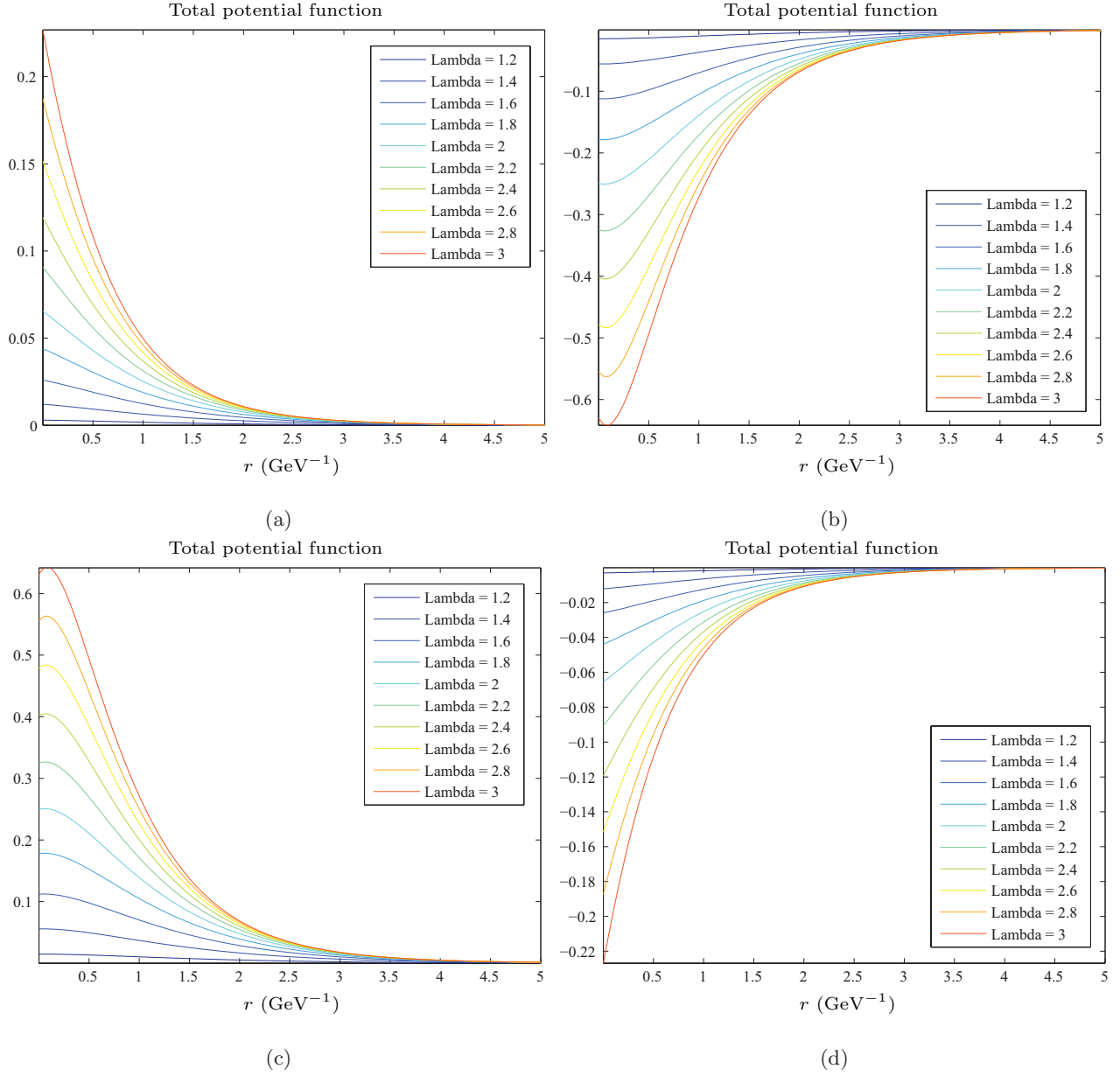


FIG. 20: (a), (b), (c) and (d) are the potentials of the  $[D^*D_0^*]_{s1}^0$  with  $(c = +1, \beta\beta' > 0)$ ,  $(c = +1, \beta\beta' < 0)$ ,  $(c = -1, \beta\beta' > 0)$  and  $(c = -1, \beta\beta' < 0)$ , respectively. Here, we take  $\zeta\varpi > 0$  with  $|\beta| = 0.909$ ,  $|\beta'| = 0.533$ ,  $|\zeta| = 0.727$  and  $|\varpi| = 0.364$ .

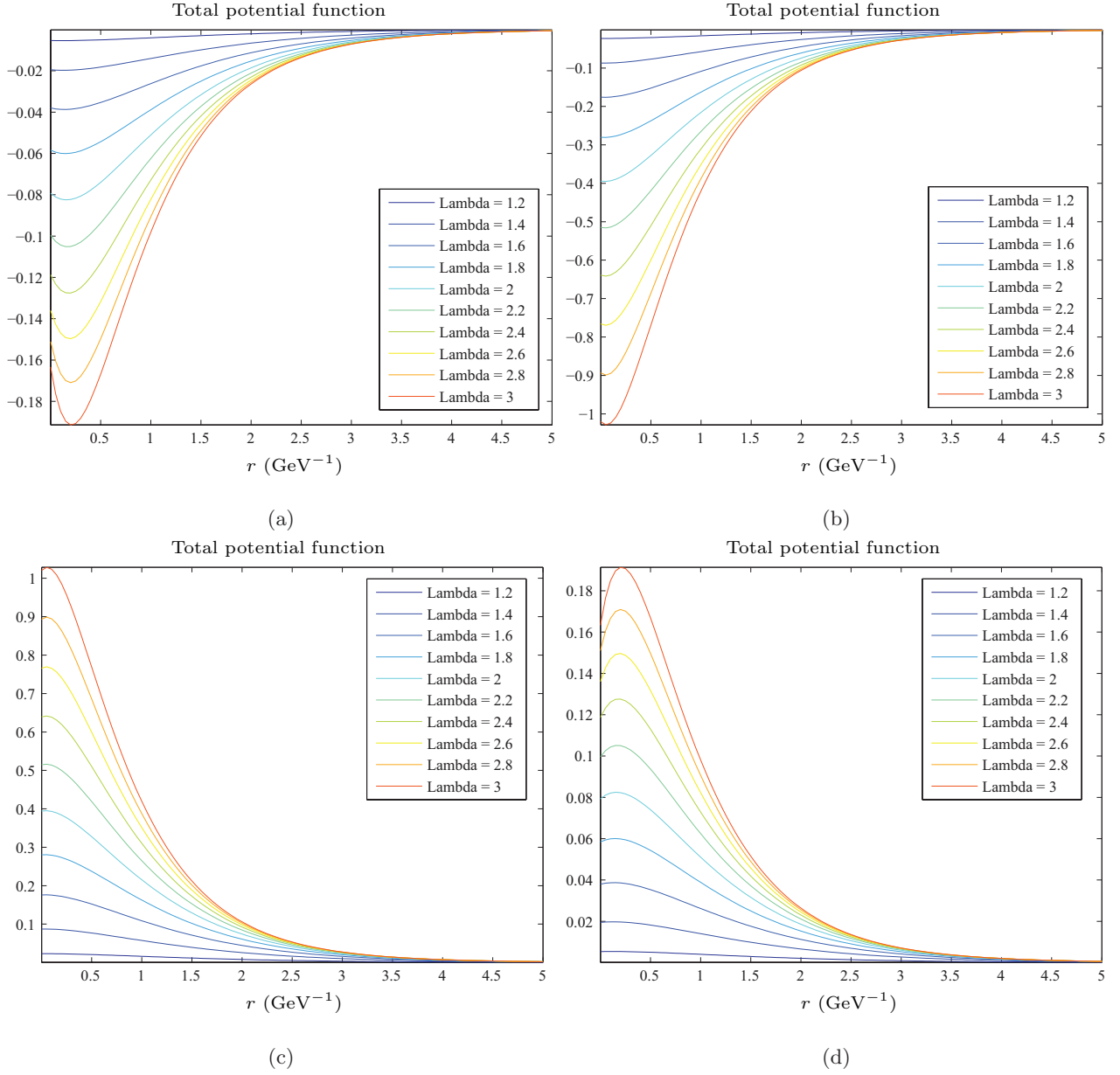


FIG. 21: (a), (b), (c) and (d) are the potentials of the  $[D^* D_0^*]_{s1}^0$  system with  $(c = +1, \beta\beta' > 0)$ ,  $(c = +1, \beta\beta' < 0)$ ,  $(c = -1, \beta\beta' > 0)$  and  $(c = -1, \beta\beta' < 0)$ , respectively. Here, we take  $\zeta\varpi < 0$  with  $|\beta| = 0.909$ ,  $|\beta'| = 0.533$ ,  $|\zeta| = 0.727$  and  $|\varpi| = 0.364$ .

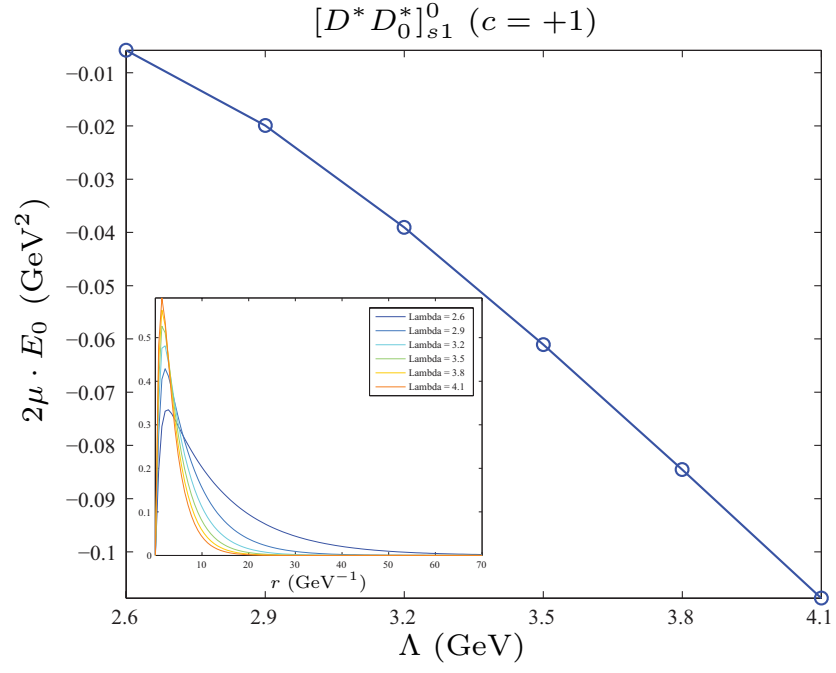


FIG. 22: The dependence of the binding energy of  $[D^* D_0^*]_{s1}^0$  on  $\Lambda$  with  $c = +1$ ,  $\beta\beta' < 0$  and  $\zeta\varpi < 0$  with  $|\beta| = 0.909$ ,  $|\beta'| = 0.533$ ,  $|\zeta| = 0.727$  and  $|\varpi| = 0.364$ .

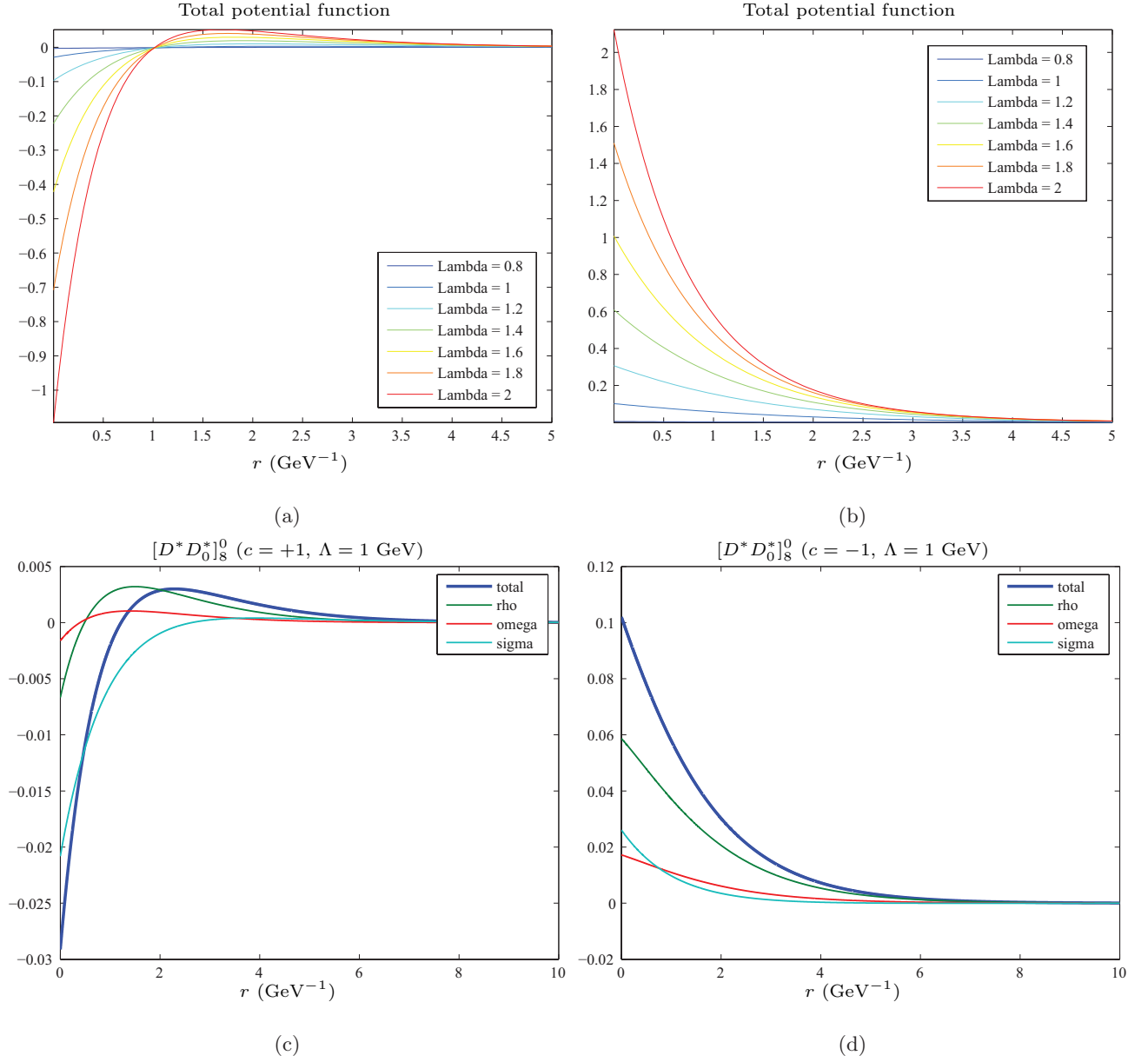


FIG. 23: (a) and (b) are the total potentials of the  $[D^* D_0^*]_8$  system with  $c = +1$  and  $c = -1$  respectively with  $g_\sigma g'_\sigma > 0$ ,  $\beta\beta' > 0$  and  $\zeta\mu > 0$  with  $|\beta| = 0.909$ ,  $|\beta'| = 0.533$ ,  $|\zeta| = 0.727$  and  $|\varpi| = 0.364$ . With  $\Lambda = 1$  GeV, we show the comparison of the total potential and the  $\sigma$ ,  $\rho$ ,  $\omega$  exchange potentials, where (c) and (d) illustrate the result of the  $[D^* D_0^*]_8$  system with  $c = +1$  and  $c = -1$  respectively.

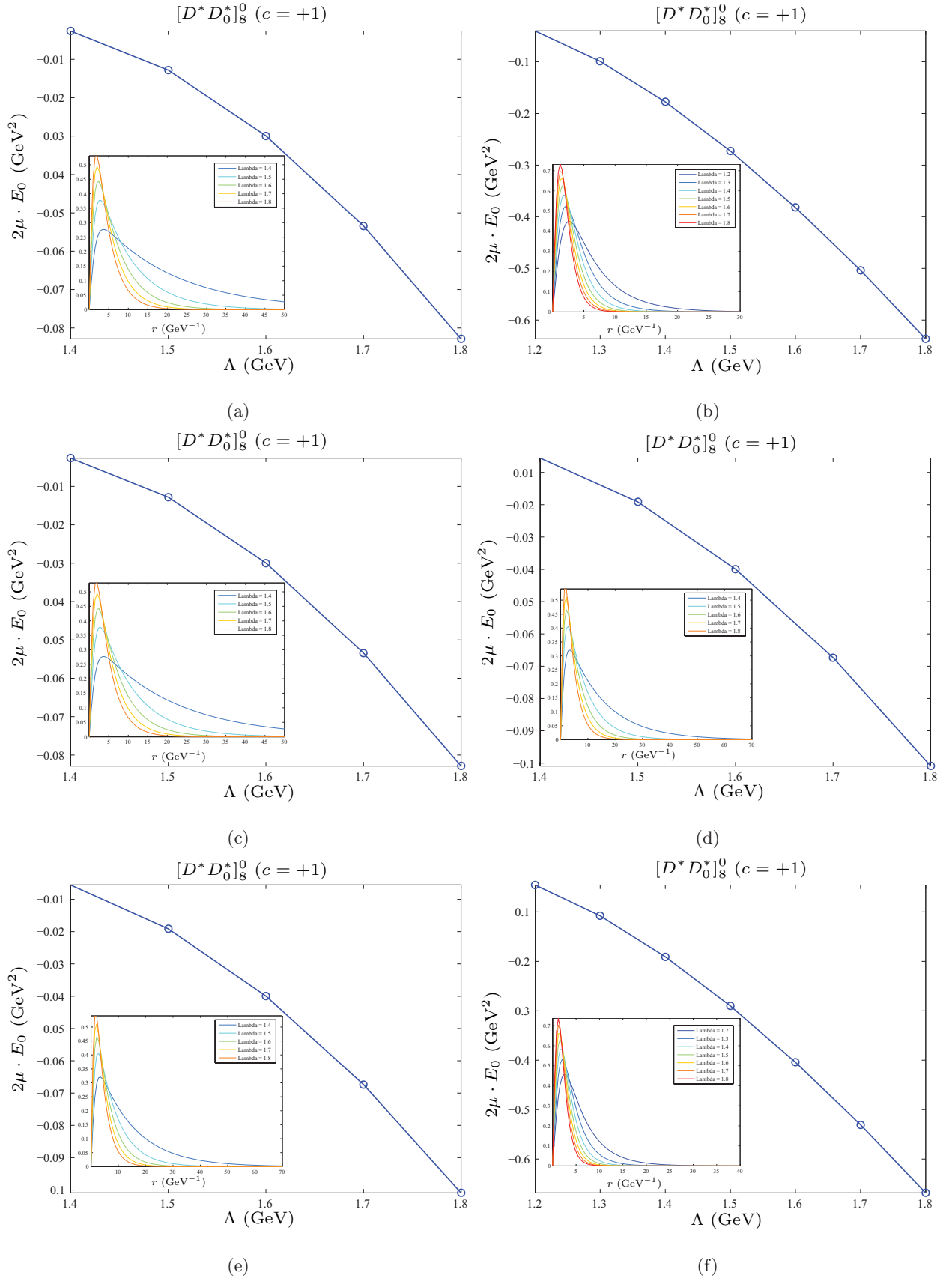


FIG. 24: The bound state solution of the  $[D^* D_0^*]_8^0$  with  $c = +1$ . (a), (b), (c), (d), (e), and (f) correspond to the results with  $(g_\sigma g'_\sigma > 0, \beta\beta' < 0, \zeta\varpi > 0)$ ,  $(g_\sigma g'_\sigma > 0, \beta\beta' < 0, \zeta\varpi < 0)$ ,  $(g_\sigma g'_\sigma > 0, \beta\beta' > 0, \zeta\varpi < 0)$ ,  $(g_\sigma g'_\sigma < 0, \beta\beta' < 0, \zeta\varpi > 0)$ ,  $(g_\sigma g'_\sigma < 0, \beta\beta' > 0, \zeta\varpi < 0)$  and  $(g_\sigma g'_\sigma < 0, \beta\beta' < 0, \zeta\varpi < 0)$  respectively. When taking  $(g_\sigma g'_\sigma > 0, \beta\beta' > 0, \zeta\varpi > 0)$  or  $(g_\sigma g'_\sigma < 0, \beta\beta' > 0, \zeta\varpi > 0)$ , we can not find the bound state solution. Here,  $|g_\sigma| = 0.76$ ,  $|g'_\sigma| = 0.76$ ,  $|h_\sigma| = 0.323$ ,  $|\beta| = 0.909$  and  $|\beta'| = 0.533$ ,  $\zeta = 0.727$  and  $\varpi = 0.364$ .

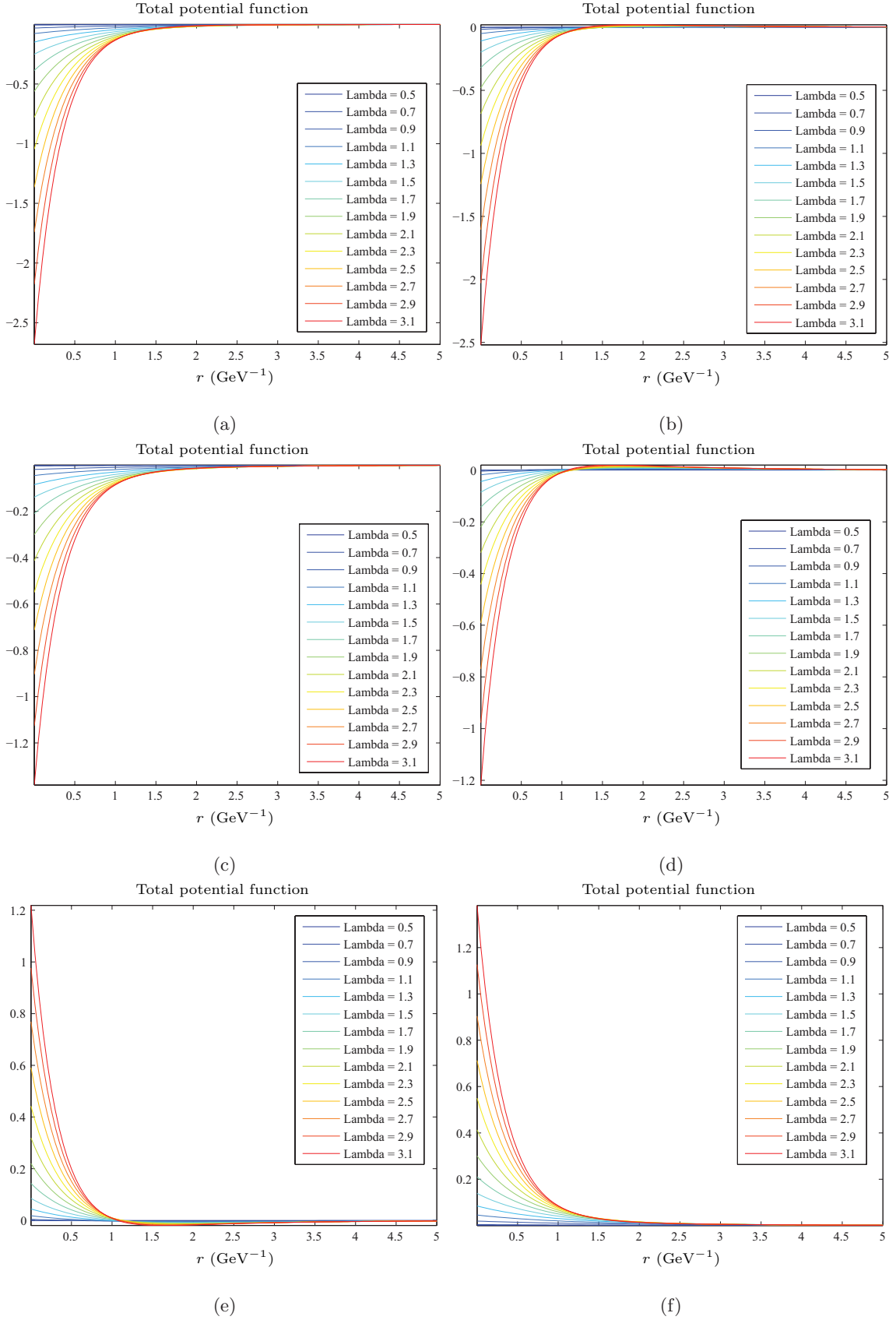


FIG. 25: The variation of the potential of the  $[D^*D_1]_{s^{\pm,0}}^{\pm,0}$ ,  $[D^*D_1]_s^0$  system, where we only list several typical cases with parameters ( $c = +1, J = 0, gg' > 0$ ), ( $c = -1, J = 0, gg' > 0$ ), ( $c = +1, J = 1, gg' > 0$ ), ( $c = -1, J = 1, gg' > 0$ ), ( $c = +1, J = 2, gg' > 0$ ) and ( $c = -1, J = 0, gg' > 0$ ), which correspond to diagrams (a), (b), (c), (d), (e) and (f) respectively. The above results are obtained with  $1h$ . Here,  $|h| = 0.56$ ,  $|g| = 0.75$  and  $|g'| = 0.25$ .

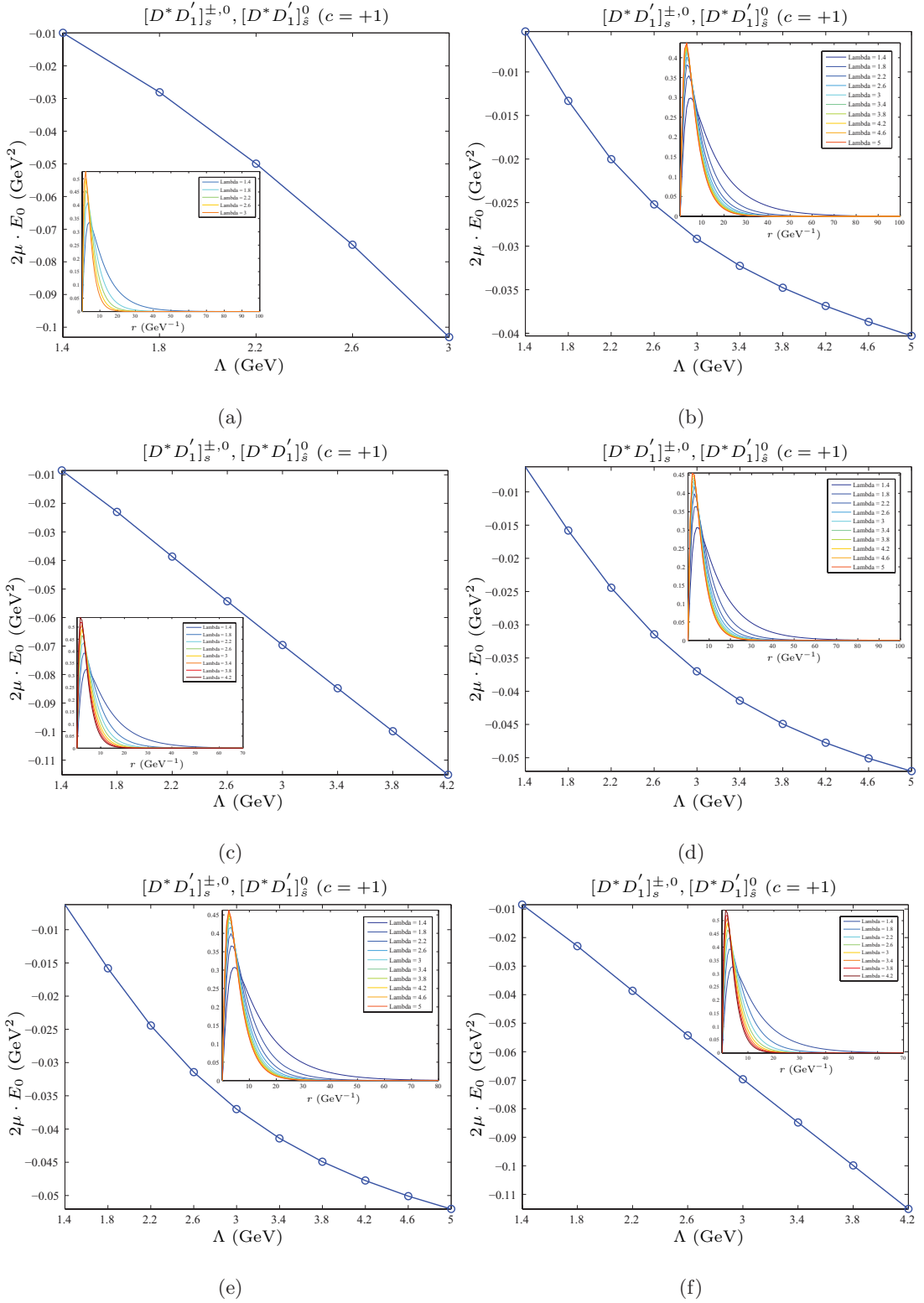


FIG. 26: The bound state solutions of the  $[D^* D'_1]_s^{\pm,0}, [D^* D'_1]_s^0$  system with ( $c = +1, J = 0, gg' > 0$ ), ( $c = +1, J = 0, gg' < 0$ ), ( $c = +1, J = 1, gg' > 0$ ), ( $c = +1, J = 1, gg' < 0$ ), ( $c = +1, J = 2, gg' > 0$ ) and ( $c = +1, J = 0, gg' < 0$ ), which correspond to diagrams (a), (b), (c), (d), (e) and (f) respectively. The above numerical results are obtained with  $3h$  while we can not find the bound state solution for  $1h$  and  $2h$ . Here,  $|h| = 0.56$ ,  $|g| = 0.75$  and  $|g'| = 0.25$ .

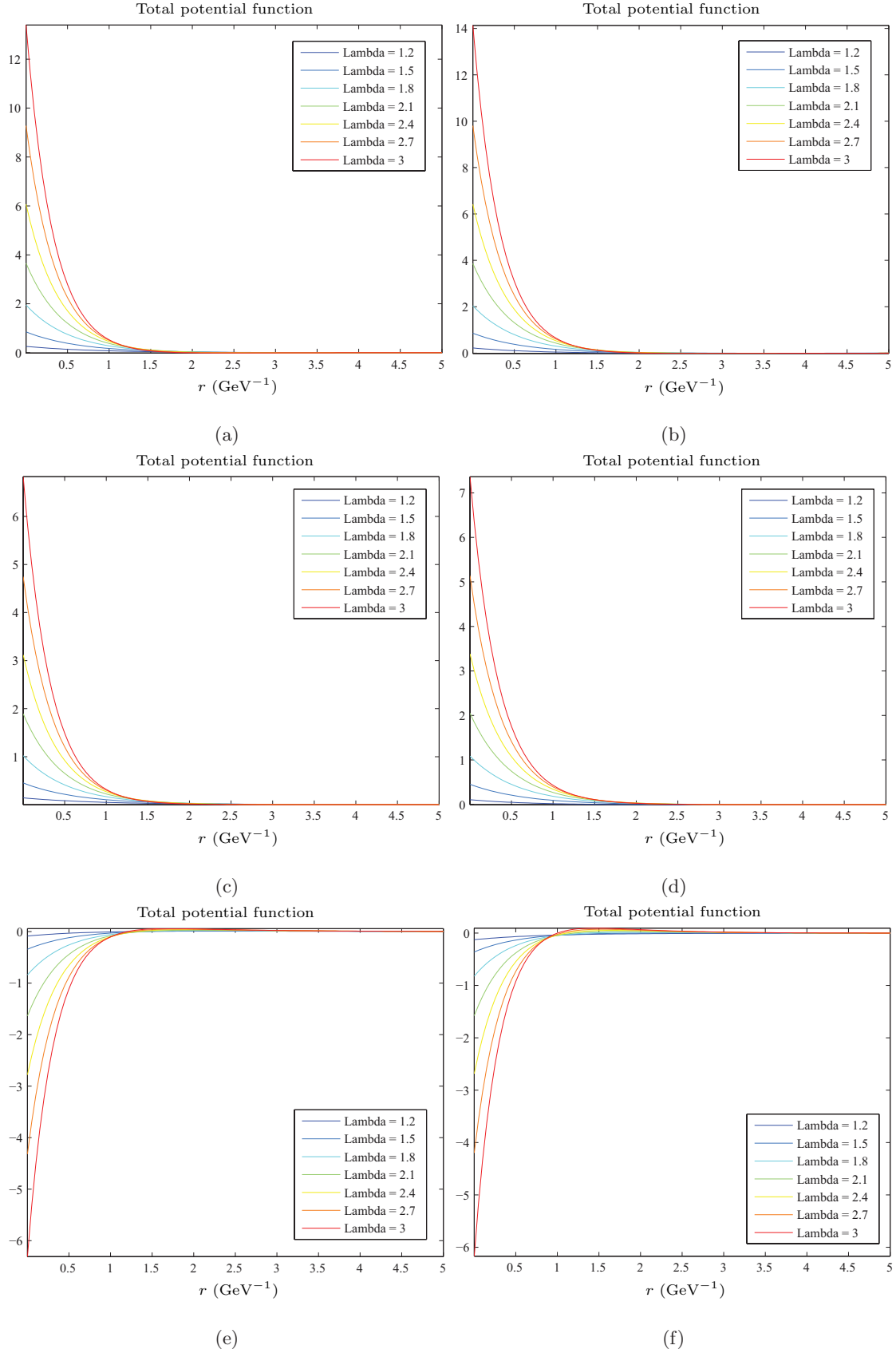


FIG. 27: The variation of the potential of the  $[D^* D_1]_{s1}^0$  system with  $r$ . (a), (b), (c), (d), (e) and (f) are for parameters  $(c = +1, J = 0, \beta\beta' > 0, \lambda\lambda' > 0, \zeta\varpi > 0)$ ,  $(c = -1, J = 0, \beta\beta' > 0, \lambda\lambda' > 0, \zeta\varpi > 0)$ ,  $(c = +1, J = 1, \beta\beta' > 0, \lambda\lambda' > 0, \zeta\varpi > 0)$ ,  $(c = -1, J = 1, \beta\beta' > 0, \lambda\lambda' > 0, \zeta\varpi > 0)$ ,  $(c = +1, J = 2, \beta\beta' > 0, \lambda\lambda' > 0, \zeta\varpi > 0)$  and  $(c = -1, J = 2, \beta\beta' > 0, \lambda\lambda' > 0, \zeta\varpi > 0)$ , respectively. Here,  $|h| = 0.56$ ,  $|g| = 0.75$ ,  $|g'| = 0.25$ ,  $|\lambda| = 0.4546$ ,  $|\lambda'| = 0.2667$ ,  $|\beta| = 0.909$ ,  $|\beta'| = 0.533$ ,  $|\zeta| = 0.727$  and  $|\varpi| = 0.364$ .

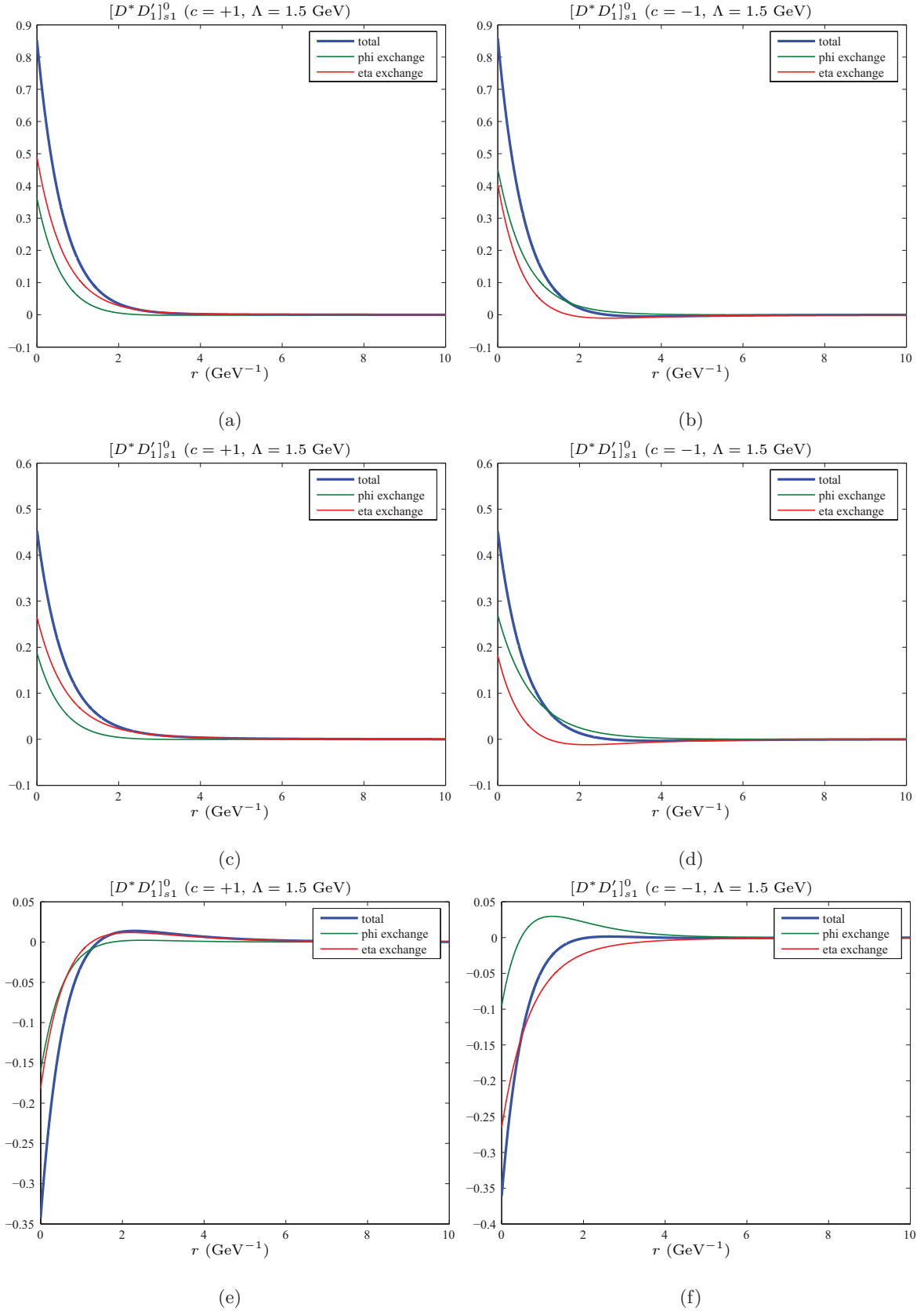


FIG. 28: The comparison of the  $\eta$  and  $\phi$  exchange potentials with the total effective potential for the  $[D^* D'_1]_{s1}^0$  system with  $\Lambda = 1.5 \text{ GeV}$ . (a), (b), (c), (d), (e) and (f) are for parameters  $(c = +1, J = 0, \beta\beta' > 0, \lambda\lambda' > 0, gg' > 0, \zeta\varpi > 0)$ ,  $(c = -1, J = 0, \beta\beta' > 0, \lambda\lambda' > 0, gg' > 0, \zeta\varpi > 0)$ ,  $(c = +1, J = 1, \beta\beta' > 0, \lambda\lambda' > 0, gg' > 0, \zeta\varpi > 0)$ ,  $(c = -1, J = 1, \beta\beta' > 0, \lambda\lambda' > 0, gg' > 0, \zeta\varpi > 0)$ ,  $(c = +1, J = 2, \beta\beta' > 0, \lambda\lambda' > 0, gg' > 0, \zeta\varpi > 0)$  and  $(c = -1, J = 2, \beta\beta' > 0, \lambda\lambda' > 0, gg' > 0, \zeta\varpi > 0)$ , respectively. Here,  $|h| = 0.56$ ,  $|g| = 0.75$ ,  $|g'| = 0.25$ ,  $|\lambda| = 0.4546$ ,  $|\lambda'| = 0.2667$ ,  $|\beta| = 0.909$ ,  $|\beta'| = 0.533$ ,  $|\zeta| = 0.727$  and  $|\varpi| = 0.364$ .

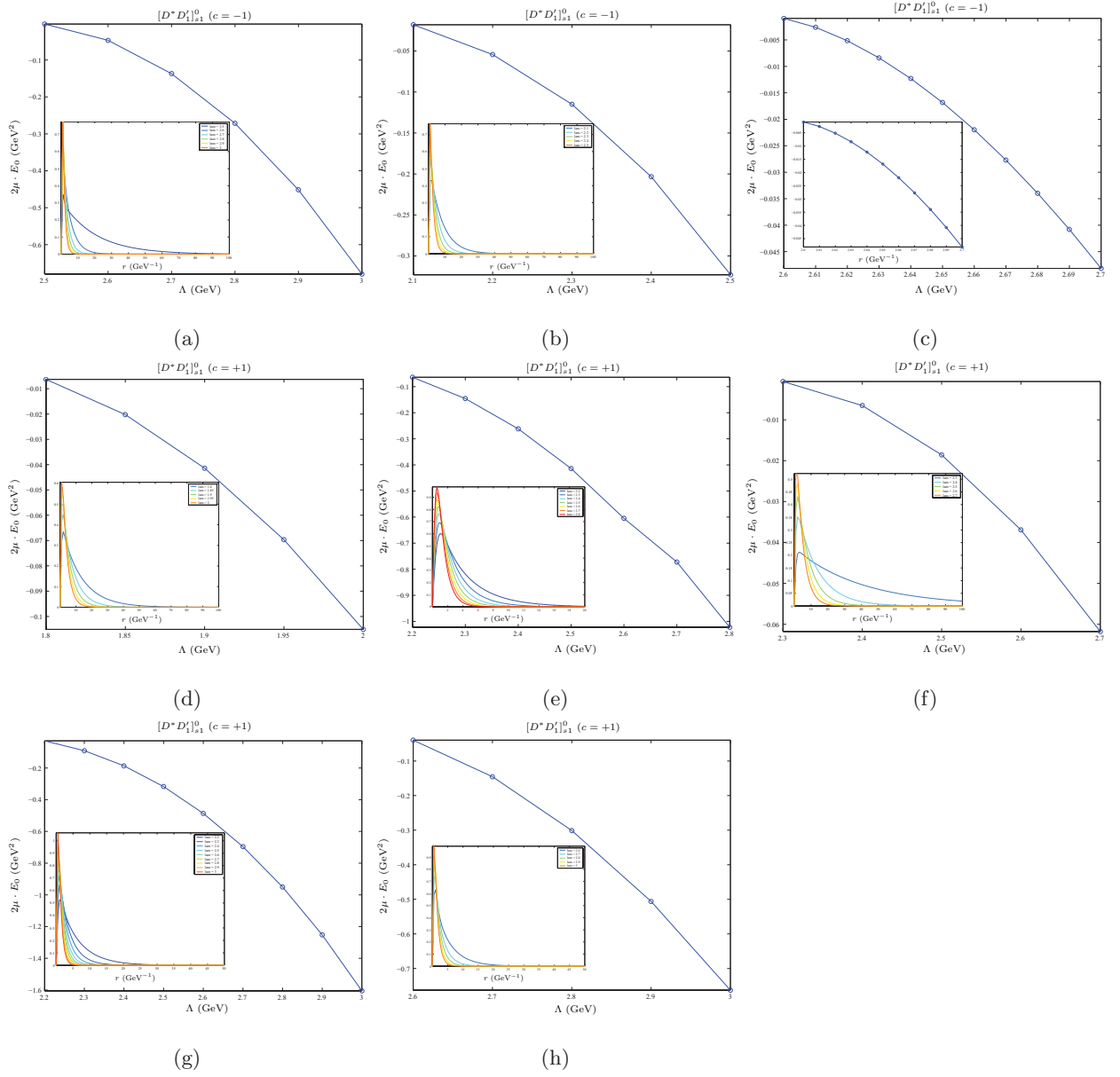


FIG. 29: The bound state solution of the  $[D^* D_1]_{s1}^0$  system with  $(c = -1, J = 0, \beta\beta' < 0, \lambda\lambda' < 0, gg' < 0, \zeta\varpi < 0)$ ,  $(c = -1, J = 0, \beta\beta' < 0, \lambda\lambda' < 0, gg' < 0, \zeta\varpi > 0)$ ,  $(c = -1, J = 0, \beta\beta' > 0, \lambda\lambda' < 0, gg' < 0, \zeta\varpi > 0)$ ,  $(c = +1, J = 0, \beta\beta' < 0, \lambda\lambda' < 0, gg' < 0, \zeta\varpi < 0)$ ,  $(c = +1, J = 0, \beta\beta' < 0, \lambda\lambda' < 0, gg' > 0, \zeta\varpi < 0)$ ,  $(c = +1, J = 0, \beta\beta' > 0, \lambda\lambda' < 0, gg' < 0, \zeta\varpi < 0)$  and  $(c = +1, J = 0, \beta\beta' > 0, \lambda\lambda' < 0, gg' < 0, \zeta\varpi > 0)$ , which correspond to diagrams (a), (b), (c), (d), (e), (f), (g) and (h) respectively. Here, we take  $1h$ .  $|h| = 0.56$ ,  $|g| = 0.75$ ,  $|g'| = 0.25$ ,  $|\lambda| = 0.4546$ ,  $|\lambda'| = 0.2667$ ,  $|\beta| = 0.909$ ,  $|\beta'| = 0.533$ ,  $|\zeta| = 0.727$  and  $|\varpi| = 0.364$ .

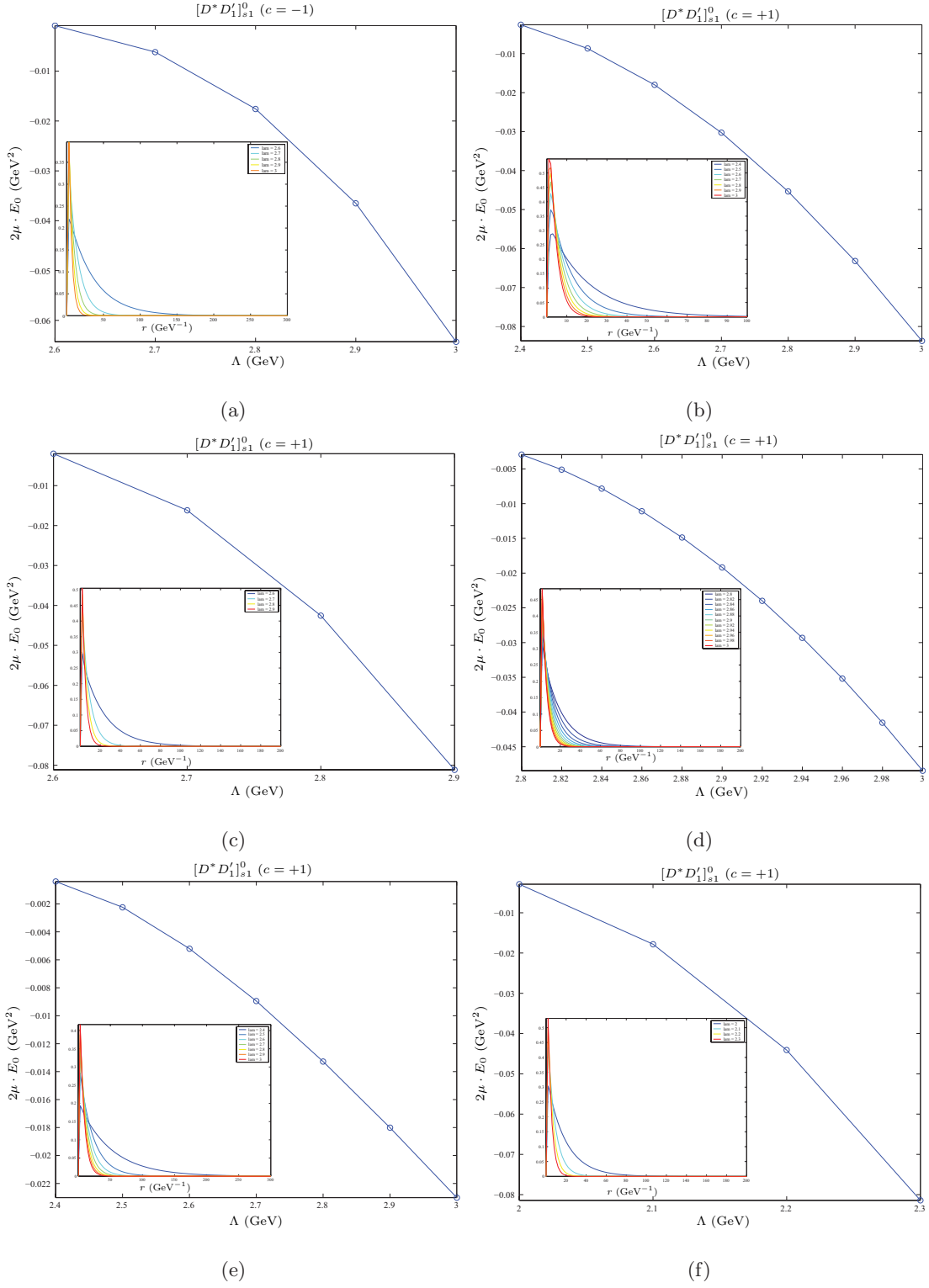


FIG. 30: The bound state solution of the  $[D^* D_1]_{s1}^0$  system with ( $c = -1, J = 1, \beta\beta' < 0, \lambda\lambda' < 0, gg' < 0, \zeta\varpi > 0$ ), ( $c = +1, J = 1, \beta\beta' > 0, \lambda\lambda' < 0, gg' > 0, \zeta\varpi < 0$ ), ( $c = +1, J = 1, \beta\beta' > 0, \lambda\lambda' < 0, gg' < 0, \zeta\varpi > 0$ ), ( $c = +1, J = 1, \beta\beta' > 0, \lambda\lambda' < 0, gg' < 0, \zeta\varpi < 0$ ), ( $c = +1, J = 1, \beta\beta' < 0, \lambda\lambda' > 0, gg' < 0, \zeta\varpi < 0$ ) and ( $c = +1, J = 1, \beta\beta' < 0, \lambda\lambda' < 0, gg' < 0, \zeta\varpi < 0$ ), which correspond to diagrams (a), (b), (c), (d), (e) and (f) respectively. Here, we use  $1h$ .  $|h| = 0.56$ ,  $|g| = 0.75$ ,  $|g'| = 0.25$ ,  $|\lambda| = 0.4546$ ,  $|\lambda'| = 0.2667$ ,  $|\beta| = 0.909$ ,  $|\beta'| = 0.533$ ,  $|\zeta| = 0.727$  and  $|\varpi| = 0.364$ .

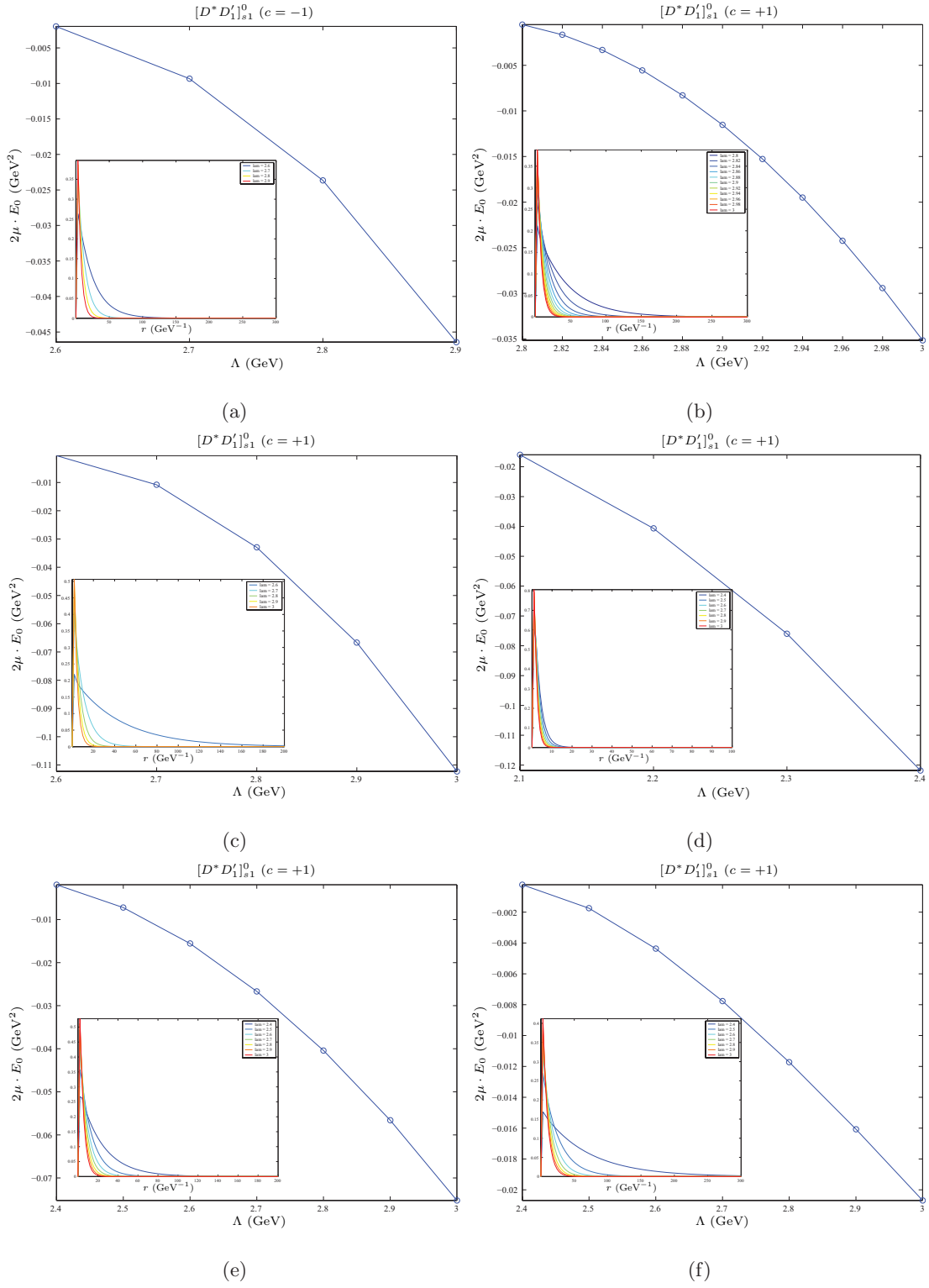


FIG. 31: The bound state solution of the  $[D^* D'_1]_{s1}^0$  system with ( $c = -1, J = 2, \beta\beta' < 0, \lambda\lambda' > 0, gg' > 0, \zeta\varpi > 0$ ), ( $c = +1, J = 2, \beta\beta' > 0, \lambda\lambda' > 0, gg' > 0, \zeta\varpi < 0$ ), ( $c = +1, J = 2, \beta\beta' < 0, \lambda\lambda' > 0, gg' > 0, \zeta\varpi > 0$ ), ( $c = +1, J = 2, \beta\beta' < 0, \lambda\lambda' > 0, gg' > 0, \zeta\varpi < 0$ ), ( $c = +1, J = 2, \beta\beta' < 0, \lambda\lambda' > 0, gg' < 0, \zeta\varpi < 0$ ) and ( $c = +1, J = 2, \beta\beta' < 0, \lambda\lambda' < 0, gg' > 0, \zeta\varpi < 0$ ), which correspond to diagrams (a), (b), (c), (d), (e) and (f) respectively. Here, we use  $1h$ .  $|h| = 0.56$ ,  $|g| = 0.75$ ,  $|g'| = 0.25$ ,  $|\lambda| = 0.4546$ ,  $|\lambda'| = 0.2667$ ,  $|\beta| = 0.909$ ,  $|\beta'| = 0.533$ ,  $|\zeta| = 0.727$  and  $|\varpi| = 0.364$ .